



Lawrence Berkeley Laboratory

UNIVERSITY OF CALIFORNIA

Materials & Chemical Sciences Division

**Electrochemical Evaluation of New Fluorosulfonic and
Fluorophosphonic Acids as Fuel Cell Electrolytes
Final Report: May 1986 – December 1989**

M.H. Saffarian and P.N. Ross

December 1989



Prepared for the U.S. Department of Energy under Contract Number DE-AC03-76SF00098.

1 LOAN COPY 1
1 CIRCULATES 1
1 FOR 2 WEEKS 1

Bldg. 50 Library.

LBL-27025 Rev

COPY 2

DISCLAIMER

This document was prepared as an account of work sponsored by the United States Government. While this document is believed to contain correct information, neither the United States Government nor any agency thereof, nor the Regents of the University of California, nor any of their employees, makes any warranty, express or implied, or assumes any legal responsibility for the accuracy, completeness, or usefulness of any information, apparatus, product, or process disclosed, or represents that its use would not infringe privately owned rights. Reference herein to any specific commercial product, process, or service by its trade name, trademark, manufacturer, or otherwise, does not necessarily constitute or imply its endorsement, recommendation, or favoring by the United States Government or any agency thereof, or the Regents of the University of California. The views and opinions of authors expressed herein do not necessarily state or reflect those of the United States Government or any agency thereof or the Regents of the University of California.

GRI-89/0060

ELECTROCHEMICAL EVALUATION OF NEW
FLUOROSULFONIC AND FLUOROPHOSPHONIC ACIDS
AS FUEL CELL ELECTROLYTES

Annual Report

January 1, 1988–December 31, 1988

Prepared by

M.H. Saffarian and P.N. Ross

Materials and Chemical Sciences Division
Lawrence Berkeley Laboratory
1 Cyclotron Road
Berkeley, California 94720

For

GAS RESEARCH INSTITUTE

Contract no. 5086-260-1229

GRI Project Manager
Daniel A. Scarpiello

Legal Notice

This report was prepared by the Lawrence Berkeley Laboratory, University of California, as an account of work sponsored by the Gas Research Institute (GRI) and supported by the Department of Energy (DOE). Neither the Government, DOE, GRI, University, nor any person acting on their behalf

- a) makes any warranty expressed or implied with respect to the accuracy, completeness, or usefulness of any information contained herein or makes any warranty that the use of such information may not infringe privately owned rights or
- b) assumes any liability with respect to the use of, or for damages resulting from the use of, any information, apparatus, method, or process disclosed in this report.

RESEARCH SUMMARY

Title ELECTROCHEMICAL EVALUATION OF NEW FLUOROSULFONIC AND FLUOROPHOSPHONIC ACIDS AS FUEL CELL ELECTROLYTES

Contractor Lawrence Berkeley Laboratory

GRI contract No. 5086-260-1229

Principal Investigator P.N. Ross

Report Period January 1, 1988 – December 31, 1988

Objective To evaluate a series of new fluorosulfonic and fluorophosphonic acid as alternative fuel cell electrolytes having superior performance than phosphoric acid.

Technical Perspective Phosphoric acid, the electrolyte currently in use in acid H_2-O_2 fuel cells, suffers from several limitations. It is desirable to identify new electrolytes that have electrochemical and physical properties superior to those of phosphoric acid such as faster kinetics for oxygen reduction, higher oxygen solubility and lower anion adsorption on the platinum catalyst. Moreover, they should possess high ionic conductivities, low vapor pressures, electrochemical and thermal stabilities and low contact angles with Teflon, characteristics of phosphoric acid.

Results A number of new fluorosulfonic and fluorophosphonic acids have been evaluated as candidates for fuel cell electrolytes. Oxygen reduction data on smooth platinum electrodes indicate that the addition of most of the new electrolytes to 85% phosphoric acid increases the oxygen solubility in the mixture. Long-chain monosulfonic acids such as $C_8F_{17}SO_3H$ are not suitable as fuel cell electrolytes due to their tendency to wet the Teflon structure of the gas diffusion electrodes. Flooding of the fuel cell electrodes has been experienced with several acids having a terminal CF_3 group. Disulfonic acids of the type $((HSO)_3)_2(CF_2)_n$ do not wet Teflon. However, the vapor pressures of acids containing only a few CF_2 groups ($n \leq 2$) are high and increasing the fluoroalkyl chain length in order to lower vapor pressure results in a decrease in their water solubilities and conductivities. Thus, even though the acid vapor pressure is low for $n \geq 3$ even at temperatures up to $200^\circ C$, the low solubility and conductivity limits the useful temperature to less than

100°C. In this homologous series, the $n = 2$ (TFEDSA) acid appeared to have the best properties as a fuel cell electrolyte, although its maximum useful operating temperature is only ca. 100°C.

The best performance from a standard Pt fuel cell cathode was obtained using a saturated aqueous solution of $(CF_3SO_2)_2CH_2$ at room temperature (!). Performance of a room temperature cell using this electrolyte was as much as 70 mV higher than an *optimized* cell using 85% H_3PO_4 at 70°C. However, optimized PAFC's running at 170–190°C produced cell voltages comparable to the room temperature $(CF_3SO_2)_2CH_2$ cell, and we found that $(CF_3SO_2)_2CH_2$ could not be used effectively at temperatures above 50°C due to limited solubility. A disulfonic acid containing an ether linkage, $[HSO_3(CF_2)_2]_2O$, showed the highest water solubility of any sulfonic acid we have examined. Short chain mono-sulfonic acids containing a terminal SF_3 group also have high water solubilities, and thus reasonable conductivities at temperatures $\geq 100^\circ C$. However, in both cases the quantities of acids provided to us were not sufficient to perform an adequate analysis of the oxygen reduction kinetics or fuel cell performance.

Technical Approach

The procedure for the evaluation of new acids was a two stage process, the first stage being physicochemical property measurements (equivalent weight, state of hydration, conductivity of aqueous solutions) and preliminary electrochemical property measurement using cyclic voltammetry. If the results in the first stage appeared promising, further electrochemical evaluation was begun using either the purified acid by itself in pH = 1 solutions (if a sufficient quantity of acid were available) or the purified acid added to pre-purified 85% phosphoric acid, and measurement of oxygen reduction kinetics either in a rotating disk electrode (RDE) cell or in a small (1 ml) fuel cell.

Project
Implications

The electrochemical evaluation of a number of new perfluorinated acid electrolytes synthesized by GRI contractors has identified several promising candidates for future research. These include disulfonic acids, $(CF_3SO_2)_2CH_2$, and $[HSO_3(CF_2)_2]_2O$. Derivatives of these acids should be prepared so that the physical chemical properties of solubility and vaporn pressure can be improved. Synthesis of higher molecular weight compounds would diminish the vapor pressure problem. The third year of this contract will continue to evaluate and characterize new acids, as they are synthesized, and recommend changes in synthetic strategy.

GRI Project
Manager

D.A. Scarpiello
Manager, Catalysis Research
Physical Sciences Department

INTRODUCTION:

A variety of fluorosulfonic and fluorophosphonic acids were evaluated in the last year. The procedure used in this evaluation was a two stage process, the first stage being physical-chemical property measurements (equivalent weight, state of hydration, conductivity of aqueous solutions) and preliminary electrochemical property measurement using cyclic voltammetry. If the results in the first stage appeared promising, further electrochemical evaluation was begun using either the purified acid by itself in pH = 1 solutions (if a sufficient quantity of acid were available) or the purified acid added to pre-purified 85% phosphoric acid, and measurement of oxygen reduction kinetics either in a rotating disk electrode (RDE) cell or in a small (1 ml) fuel cell.

EXPERIMENTAL:

All electrolytes were prepared either with Harleco ultra-pure water or with highly pure water obtained by circulating distilled water through Milli-Q (Waters) water purification unit. Purity of newly synthesized acids was checked by recording cyclic voltammograms in dilute acid solutions having pH = 1. Different platinum electrodes and cell configurations were used in cyclic voltammetric measurements. Preliminary experiments were conducted either on a platinum cylinder electrode or on platinum flags of different sizes. The selection of a given electrode was based on the quantity of the sample supplied by the synthetic chemist. Several glass cells were fabricated in order to accommodate various solution volumes ranging from 1 to 200 milliliters. A large (compared to working electrode) platinum flag served as counter electrode. In oxygen reduction experiments, this electrode was directly inserted into the cell solution. The potential of the working electrode was monitored with respect to a dynamic hydrogen electrode (DHE) in a separate compartment, connected to the main cell via a luggin capillary. A

reversible hydrogen electrode (RHE) requiring only 0.5 ml of solution, was used for samples which were supplied in small quantities. This reference electrode was filled with the test solution and then hydrogen was electrochemically generated at the platinumized platinum electrode.

In oxygen reduction kinetics measurements, two different cells and conditions were used. For purified solutions of the acids, nominally pH 1 were examined in a 200 ml glass cell. A standard Pine Instruments Pt RDE and Pine rotor were used. Measurements of acid mixtures with 85% phosphoric acid were done in a small Teflon fuel cell with 1 cm² active area commercial fuel cell Pt Electrodes (Prototech). The temperature for the fuel cell data was typically 100°C. Some acid mixture experiments were also performed in the RDE cell by adding the new acids to 0.7M or 0.1M phosphoric acid solutions.

Purity of the new acids was tested by recording a cyclic voltammogram in dilute aqueous solution (pH 1) and comparing the results with that of purified phosphoric or sulfuric acid. This was done before each of the "super acids" was tested.

A PAR 273 or Pine RDE4 potentiostat/galvanostat was used in cyclic voltammetry experiments. Rotating disk electrode and fuel cell data were collected by PAR 273 in the remote mode, using an IBM PC as the host computer.

The results of cyclic voltammetry experiments are described in the following section. All acids received for electrochemical evaluation are listed in Table 1. The geometrical areas of electrodes used: 6.8 cm² (Figs. 2,9,12), 3.96 cm² (Figs. 3,6,8,14), 3.76 cm² (Figs. 10,11,13,15) and 0.05 cm² (Actual, Figs. 4,5).

A- CYCLIC VOLTAMMETRY DATA:

Figure 1 illustrates the rotating cylinder electrochemical cell. The cell requires only 30 ml of solution, suitable for electrochemical evaluation of new super acids. The large ratio of surface area (6.8 cm^2) to electrolyte volume was intended for minimizing the effect of impurities. Although this was true for the stationary electrode, the quality of oxygen reduction kinetics data was lower than those obtained using a rotating disk electrode.

Figure 2 shows cyclic voltammogram of Pt in purified 0.7M (pH 1) phosphoric acid solution saturated with purified nitrogen. This voltammogram was used for the comparison of Pt behavior in the new super acids. The well-defined oxide formation and reduction regions and symmetrical hydrogen adsorption-desorption peaks are typical of a solution free from any adsorbable or electroactive impurities. Cleanliness of electrode and cell assembly was also checked with 0.1N sulfuric acid. The corresponding cyclic voltammogram is shown in figure 3.

Figure 4 and 5 show the cyclic voltammograms of Pt in 0.18M solution of $\text{CF}_3(\text{CF}_2)_2\text{CH}_2\text{OCF}_2\text{CF}_2\text{SO}_3\text{H}$ and 0.25M solution of $\text{CF}_3\text{CH}_2\text{OCF}_2\text{CF}_2\text{SO}_3\text{H}$, saturated with N_2 , respectively. These acids were received from the University of Idaho as yellow-brown liquids of less than 1g each. These solutions had a strong odor. Significant amount of impurities were present in each acid. Considering the small quantities provided, no purification procedure was attempted.

Cyclic voltammogram of Pt in 0.016M solution of $(\text{CF}_3\text{SO}_2)_2\text{CH}_2$ is shown in Figure 6. This acid was received as a crystalline white solid. The sample was less than one gram. Cyclic voltammetry data indicates the presence of some oxidizable impurities in the solution. Because of small amount of material available, no further study was

conducted.

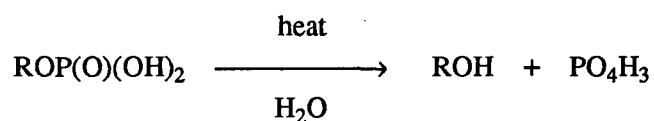
Figure 7 shows the voltammogram of 0.1N (0.05M) solution of $(\text{HO}_3\text{S}(\text{CF}_2)_2)_2\text{O}$ saturated with N_2 . This acid was received as a viscous clear liquid. The equivalent weight was determined to be 178. Based on the molecular formula, the equivalent of an anhydrous sample would be 189. The discrepancy indicates the presence of a significant amount of a lower molecular weight acid. Cyclic voltammetric data indicate that the sample contains considerable amount of impurities. Several grams of acid were available, so a purification procedure was done.

The acid was treated with hydrogen peroxide and refluxed at 80°C for several hours. The solution was then boiled down to a viscous liquid which solidified upon cooling to a white gelatin. A small amount of liquid was present. The equivalent weight of purified acid was measured to be 181. This indicates that some of the lower molecular weight acid has been preferentially removed, but significant amounts likely remained. Cyclic voltammogram of Pt after purification is shown in figure 8, indicating that a significant improvement has been achieved. The amount of acid left after first purification, was just enough to be used as an additive to 85% phosphoric acid for fuel cell testing. Results of the fuel cell experiments will be shown in section C.

Cyclic voltammetry of Pt in 0.05M (based on the theoretical formula weight) solution of $(\text{HO})_2\text{P}(\text{O})\text{OCH}_2(\text{CF}_2)_4\text{CH}_2\text{OP}(\text{O})(\text{OH})_2$ is shown in figure 9. The measured pH of this solution was ca. 1.2. The solution as-prepared contained tiny droplets of "oil" which settled out after a few hours and were removed. Appearance of a peak at 0.85 V, the shapes of oxide formation/reduction waves and poor resolution of hydrogen adsorption regions are clear evidence for an impure electrolyte. No significant improvement was produced by cycling for a few hours, or by constant current electrolysis with Pt electrodes at $5\text{mA}/\text{cm}^2$ for 2 days. While purging the solution with N_2 to remove

dissolved hydrogen and oxygen and recording cyclic voltammogram, a vigorous reaction started suddenly which rapidly heated the solution to ca. 70°C.

Hydrogen peroxide treatment was applied in order to purify this acid. After removing excess water, a two-phase viscous solution containing a small amount of a crystalline material was obtained. It is known that perfluorinated alkylphosphonic acids are hydrolytically unstable, specially at high temperatures, and decompose to the corresponding alcohol according to the following reaction:



Our observations can be explained on the basis of such a decomposition reaction.

Two samples of two monosulfonic acids, each containing a terminal SF₅ group were supplied by Prof. Gard of Portland State University as white solids. The cyclic voltammogram of Pt in 0.1M solution of SF₅CH₂SO₃H is shown in figure 10. This sample is reasonably clean and the small amount of impurities can be easily removed by hydrogen peroxide treatment. Figure 11 illustrates the voltammogram of Pt in 0.118M solution of SF₅CHFCF₂SO₃H. Both solutions were readily dissolved in water and have high proton conductivities. Larger quantities of these acids were requested for further investigations.

A sample of disulfonic acid, (CF₂)₆(SO₃H)₂, referred to hereafter as C₆, was received as a white solid from Portland State University. The equivalent weight of the acid as-received was determined by titration to be 535. An aqueous 0.05M solution of was prepared, having a measured pH of 1.18. The cyclic voltammetry curve for this solution is shown in figure 12. After 48 hours of continuous cycling, the appearance of

the voltammetry curves improved considerably (curve B), characteristics of removal of oxidizable impurities. The conductivity of 0.05M solution saturated with air at 90°C was 55 mmhos, a much higher conductivity than a pH 1 solution of TFEDSA at the same conditions. This acid was considered to be promising and a larger quantity was requested from PSU, and both one-stage and two-stage purification was carried out. The cyclic voltammogram of Pt in the purified 0.05M solution is shown in figure 13. The current in the oxide formation region is still high indicating the presence of some impurities. It seems that this one-stage purification procedure is not sufficient enough to remove all impurities. Subsequently, we adopted a two-stage purification procedure which is described below in Section B.

A long-chain monosulfonic acid, $C_8F_{17}SO_3H$, referred to hereafter as C_8 , was received as a white powder. The equivalent weight was determined to be 533 by titration with 0.01N sodium hydroxide solution. A 50 ml 0.091N solution of this acid was prepared. The measured pH of this solution was 1.1. This solution was extremely foamy, making difficult simple procedures such as purging with nitrogen. A cyclic voltammogram of 0.091N solution of this acid is shown in Figure 14. This is one of the highest quality voltammograms which we have observed in the synthesized acids. This acid was purified by hydrogen peroxide treatment. A viscous liquid was obtained after heating the solution in order to remove the excess water. The concentration of this solution was found to be 1.2M by titration. If heating is continued, a "crystalline liquid" is formed. Figure 15 shows the cyclic voltammogram of 0.1N solution after purification which indicates the sample is reasonably clean.

A sample of the perfluorinated acid, $(CF_2)_4(SO_3H)_2$ was received from Prof. Gard as a white solid and a 0.1M solution of this acid was prepared. Figure 16 shows the cyclic voltammogram of Pt in 0.1M solution of $(CF_2)_4(SO_3H)_2$ saturated with nitrogen.

Although the voltammogram is fairly clean, the presence of some impurities is evident from the high currents in the oxide formation region and the relatively poor resolution of the hydrogen adsorption/desorption peaks.

This acid was purified by H_2O_2 and H_2/Pt black treatment as described in previous reports. The voltammogram of Pt in 0.1M purified solution of $(\text{CF}_2)_4(\text{SO}_3\text{H})_2$ is shown in figure 17. There are distinct symmetrical adsorption/desorption peaks and the oxide formation region is well-defined, indicating that most of impurities have been removed from the solution by the purification process. The starting potential for platinum oxide formation has been shifted to more cathodic potentials (relative to H_3PO_4 at same pH) due to the weaker interaction or adsorption of this acid on platinum surface.

Figure 18 shows the cyclic voltammogram of Pt in 0.1M solution of $(\text{CF}_3\text{SO}_2)_2\text{CH}_2$ saturated in N_2 . The voltammogram, which is similar to the one reported previously, indicates the presence of impurities in the solution. In the oxide formation region, an additional peak appears at about 1.2V (vs RHE) which is due to the presence of some oxidizable impurities in the electrolyte. The hydrogen adsorption/desorption peaks are not distinct either. These observations suggest that the solution is contaminated. Cyclic voltammogram of the same electrolyte, after purification is shown in figure 19. A significant improvement has been achieved by the two-stage purification process. As in the case of $(\text{CF}_2)_4(\text{SO}_3\text{H})_2$, the growth of oxide layer starts at a lower potential compared to phosphoric acid, indicating a lower tendency for adsorption on the platinum electrode than phosphoric acid.

B: OXYGEN REDUCTION KINETICS MEASUREMENTS

All electrolytes were purified with H_2O_2 and H_2 -Pt black treatment as recommended by CWRU. Except for the filtration of Pt black, Teflon (PFA) bottles were

used in order to minimize the solution contact with glass. A significant improvement on the purity level of 85% H_3PO_4 was observed when compared to a single-stage hydrogen peroxide treatment. In the case of C_8 acid (and C_6 , to a lesser extent), some problems were encountered. The aqueous solution of this acid acts as a strong surfactant. Decomposition of hydrogen peroxide was quite slow due to the formation of a very tiny gas bubbles which continued to evolve for several days and formed a foam layer on the top of the solution.

For all measurements a rotating disk electrode (geom. area = 0.46 cm^2) was used. The electrode was polished with alumina (final stage, $0.05 \text{ }\mu\text{m}$) to a mirror finish. It was washed, degreased, cleaned in 1:1 $\text{HNO}_3/\text{H}_2\text{SO}_4$ and finally rinsed thoroughly with ultrapure water. A reversible hydrogen electrode, filled with the test solution served as the reference electrode. A platinum flag was used as counter electrode.

The activity of smooth platinum for oxygen reduction was tested in 0.1M solution of C_6 and the results were compared to those obtained for 0.1M phosphoric acid. The electroreduction of oxygen in 85% H_3PO_4 containing low concentrations of C_6 and C_8 were also carried out. Cyclic voltammetry and rotating disk electrode techniques have been used to study the effect of the perfluorosulfonic acids as additives to 85% H_3PO_4 on the oxygen reduction on smooth Pt.

Cyclic voltammogram of Pt in purified 0.1M phosphoric acid is shown in figure 20 as a reference for comparison. It has all the characteristics of an impurity-free electrolyte. Figure 21 shows the cyclic voltammogram of Pt in a 0.1N solution of unpurified C_6 acid saturated with N_2 . The shape of the voltammogram indicates the presence of impurities in the solution. The current in the oxide formation region is higher than expected and the hydrogen adsorption-desorption peaks are completely

suppressed. A brown thin film was formed on the electrode surface when the potential was cycled between 0.02V to 1.5V for few hours. This film which was not dissolved in 1:1 HNO₃/H₂SO₄, was similar to the one reported previously when a Pt cylinder electrode with a higher surface area was used. The cyclic voltammogram of Pt in purified (twice) 0.087N solution of C₆ is shown in figure 22. No film formation was experienced in the purified solution indicating that this was due to the presence of impurities in the original solution. The shape of the peaks in the oxide and hydrogen adsorption-desorption regions of figure 22 are indicatives of a much cleaner solution. In figure 23, the voltammograms for the two purified acids are compared directly. The oxide formation in the dilute C₆ acid solution starts at a more cathodic potential and the currents for both oxide formation region and its reduction are higher relative to dilute phosphoric acid. This is the result of the weaker adsorption of the sulfonic acid compared to phosphoric acid.

Figures 24 and 25 show the cyclic voltammograms of Pt in O₂ saturated solutions of 0.1M H₃PO₄ and 0.087N (CF₂)₆(SO₃H)₂ respectively. The electrode was activated by applying potential pulses between 0.2V and 1.2V. The potential then stepped to 1.2V and scanned cathodically at 10 mV/s. The first as well as the third cycle (steady-state) is shown for each solution. Although the onset of the oxygen reduction starts at more anodic potential for sulfonic acid, the peak potential shifts in the cathodic direction and peak intensity decreases. This might be due to the traces of impurities left in the solution. For H₃PO₄ solution, the peak potential remains constant while its intensity increases upon cycling. The steady-state peak intensities are almost the same for both solutions, indicating the comparable oxygen solubilities in the dilute solutions.

Oxygen reduction experiments also were carried out in pure 85% H₃PO₄ and a mixture containing 0.45% (CF₂)₆(SO₃H)₂ in 85% phosphoric acid. The corresponding

cyclic voltammograms in the O_2 saturated H_3PO_4 solutions before and after the addition of C_6 acid are shown in figure 26.

The polarization curves were recorded at different rotation rates as indicated in figure 27 for 85% H_3PO_4 . The electrode was activated by application of 5 pulses (20 sec.) between 0.2V and 1.5V, then the potential stepped to 1.0V and I-E curves recorded at 10 mV/s in the cathodic direction. The slight increase observed in the limiting disk currents at $E < 0.35V$ results from initial adsorption of hydrogen, as can be seen by reference to figure 26.

After recording I-E curves in 85% H_3PO_4 , solid C_6 acid was added to the cell. The concentration of C_6 acid was found to be 0.45%. The low concentration was chosen because the solubility of C_6 acid in 85% H_3PO_4 is quite low and foam formation at higher concentrations makes the measurement less reliable. The mixture was purged with oxygen overnight at a low rate due to formation of foam bubbles. As figure 26 shows, there is no significant difference upon the addition of C_6 to H_3PO_4 at this low concentration. Polarization curves for oxygen reduction in the mixture were recorded following the same procedure described for H_3PO_4 . It can be seen that limiting currents for the mixture in figure 28 are higher at all rotation rates in the presence of C_6 acid. This is due to the higher oxygen solubility in the mixture relative to 85% phosphoric acid. On the other hand, the onset of oxygen reduction in the mixture coincides with that in pure phosphoric acid and no cathodic shift in the reduction potential was observed, as might be expected from an enhancement in kinetics.

We also examined the effect of on the kinetics of oxygen reduction in 0.7M phosphoric acid with the RDE. In particular, we wanted to see if there were an increase in the limiting current with C_8 addition, indicative of higher oxygen solubility. Figures 29 and 30 compare the results in purified phosphoric acid after addition of the as-

received C_8 to a level of 0.01M. Formation of huge amount of foam makes the measurement unreliable at high rotation rates. Although the limiting currents are not much different at low rotation rates, the kinetics currents are clearly lower in the mixture.

Oxygen reduction kinetics in a purified 85% phosphoric acid solution was compared with that of C_8 acid as an additive (0.45%). The corresponding voltammograms are shown in figure 31. The currents in the Pt oxidation and reduction regions are slightly higher in the mixture. The oxygen solubility in 85% H_3PO_4 increases upon addition of C_8 , as seen by comparing the magnitude of the limiting current at 400RPM in the polarization curves shown in figures 27 and 32. Formation of foam bubbles which forces the solution out of cell makes the measurements at higher rotation rates unreliable. Therefore, polarization curves for the mixture were recorded only at 100 and 400 RPM, shown in figure 32. Although the limiting current at 400 RPM is higher for the mixture than for pure H_3PO_4 the oxygen reduction potentials have been shifted quite significantly to more cathodic potentials, even though C_8 concentration in the mixture is low. The same phenomenon has been previously observed in 0.7M H_3PO_4 solution containing 1% C_8 acid. Due to the availability of small quantity of purified C_8 acid, it was used only as an additive. However, it clearly has no beneficial effect on O_2 reduction kinetics as an additive to H_3PO_4 .

Kinetics of oxygen reduction was studied at a stationary Pt disk electrode in dilute (0.1M) solution of $(CF_2)_4(SO_3H)_2$ and $(CF_3SO_2)_2CH_2$ saturated with oxygen and the results were compared with the data obtained in 0.1M H_3PO_4 under identical conditions. Before recording each voltammogram, the electrode was pulsed between 0.05 to 1.4 V. Then the cyclic voltammogram (only the first cycle) was recorded at 10 mV/sec, starting at 1.0 V. The experiment was repeated three times, and the average of the three runs is shown in figure 33 for phosphoric acid. Figures 34 and 35 show the

corresponding voltammograms for $(CF_2)_4(SO_3H)_2$ and $(CF_3SO_2)_2CH_2$ respectively. *The peak potential for oxygen reduction in 0.1M $(CF_2)_4(SO_3H)_2$ has been shifted by 55 mV to a more anodic potential (lower polarization) compared to phosphoric acid.* The peak current density is also slightly higher than the corresponding value in 0.1M H_3PO_4 . The kinetics of oxygen reduction in $(CF_3SO_2)_2CH_2$ is even better than that of $(CF_2)_4(SO_3H)_2$ solution. *The anodic shift for oxygen reduction in this solution is 75 mV relative to 0.1M H_3PO_4 and the peak current density has been increased further.*

Similar results were obtained when a Pt rotating disk electrode was used. Figures 36–38 show the results of oxygen reduction measurements at rotation rates of 400, 900 and 1600 RPM. At any given potential in the kinetics region, the oxygen reduction current is higher in 0.1M $(CF_3SO_2)_2CH_2$ than in 0.1M H_3PO_4 or even in 0.1M $(CF_2)_4(SO_3H)_2$ and the oxygen reduction starts at less cathodic potentials definitely indicating *a higher activity of Pt for oxygen reduction in this perfluorinated acid.*

C- FUEL CELL MEASUREMENTS

Fuel cell experiments were conducted in a small Teflon cell. Electrodes were high surface area standard fuel cell type (Prototech) electrodes with 1 cm^2 active area. Polarization curves were recorded at 100°C using pure hydrogen and oxygen at atmospheric pressure.

The effect of $C_8F_{17}SO_3H$, as additive to 85% phosphoric acid, on the performance of the fuel cell cathode was investigated for mixtures containing 0.5% to 25% of the as-received monosulfonic acid. It was not possible to collect any meaningful data in the concentration range of 2% to 25%. The oxygen reduction reaction became mass-transport controlled immediately after the application of a galvanostatic pulse, even at low current densities. At the same time, the cell resistance increased from 1.6 ohm in

pure phosphoric acid to 2.6 ohm for the 25% sulfonic acid in the mixture. By lowering the concentration of C_8 to 0.5%, a measurable gain in potential was observed when a galvanostatic sweep of 2 mA/sec was applied to the cell, as seen from the I-E curves in figure 39. Cell potentials were corrected for IR drop by measuring the cell resistance using either a Wayne Kerr bridge or current interrupt technique. Increasing the sulfonic acid concentration to 1% in the mixture resulted in an increase in the cathode polarization. The fuel cell performance was deteriorating with time, which was probably due to the flooding of the electrode structure. Additional experiments were performed in purified solutions but similar problems were experienced. No reliable data could be collected when purified 45% C_8 was introduced into the cell, because of continuous drifting of the cell potential. The cell resistance started to increase with time and would reach as high as 250 ohms. Addition of fresh acid would decrease the cell resistance for a short period of time. Titration of the "gel" remained in the cell after few hours of operation indicated loss of water from the cell which, in turn, resulted in a lower conductance. A layer of detergent was found on the gas side of the oxygen cathode as the result of wetting of the the Teflon structure of the electrode.

Solubility of the C_6 acid in water is quite low (0.1M) and its aqueous solutions are not suitable for fuel cell testing at high temperatures. The results of fuel cell measurements for a 1% solution of C_6 in 85% phosphoric acid were not different from the data collected in pure 85% H_3O_4 , within the experimental error. Figure 40 shows the current-potential data in the range of 0.01 to 100 mA, collected point-by-point in 85% phosphoric acid containing 2% disulfonic acid. It indicates that addition of C_6 to phosphoric acid slightly lowers the fuel cell performance.

Figure 41 shows the polarization data for oxygen reduction in purified phosphoric acid containing 1.3% $[HSO_3(CF_2)]_2O$. The cathode polarization was lower by

about 10 mV at currents greater than 1 mA. There was not enough sample available to study the fuel cell performance of the pure acid or as additive to phosphoric acid at other concentrations. Synthesis of more acid at the University of Idaho was requested.

The polarization curves for 85% phosphoric acid at 100°C and for saturated solution of $(CF_2)_4(SO_3H)_2$ at room temperature (22°C) are shown in figure 42. Room temperature performance of the cell in the presence of the disulfonic acid is comparable to, or even better at 1–20 mA) than that of phosphoric acid at 100°C up to 50 mA. At >50 mA, the reaction becomes mass-transfer controlled and the current drops sharply. Similar data are plotted in Figure 43. In this case, the polarization curve of phosphoric acid at 70°C is used as a reference. From Fig. 43, it is clear that the overpotential for oxygen reduction is lower over the entire range (especially in the current range of 2–50 mA) by 40 mV. *This is due to the higher activity of Pt for oxygen reduction as well as to higher oxygen solubility in aqueous $(CF_2)_4(SO_3H)_2$ as compared to concentrated phosphoric acid.* However, the conductivity of $(CF_2)_4(SO_3H)_2$, is much lower than that for $(CF_2)_2(SO_3H)_2$, so that the latter is the best electrolyte of the acids in the $(CF_2)_n(SO_3H)_2$ homologous series.

The oxygen reduction overpotential was even lower when a saturated aqueous solution of $(CF_3SO_2)_2CH_2$ was used. The fuel cell performance is compared in figures 44 and 45 with that of phosphoric acid at different temperatures. The room-temperature cell potentials in $(CF_3SO_2)_2CH_2$ are significantly higher (40–50 mV) in the entire current range studied compared to those of phosphoric acid at 70°C. The lowering of the overpotential in the current range of 1µA–10mA is evident even when the polarization data are compared with those of H_3PO_4 at 100°C. The open circuit potential of 1042 mV is the highest value measured for all fluorinated acids that we have evaluated

so far. Most importantly, the conductivity of the saturated solution of this acid *at room temperature was the highest of any fluorinated acid we have evaluated so far.*

D: CONDUCTIVITY MEASUREMENTS

Specific conductivities have been measured for a number of new acids using a Wayne Kerr Autobalance Universal Bridge B642, over a temperature range between 25 to 90°C. Temperature of air saturated solutions was controlled to + 0.5°C using a water bath. The measured conductivity data for 0.05 M (pH 1) solutions of $(CF_2)_6(SO_3H)_2$ and $[(OH)_2P(O)OCH_2(CF_2)_2]_2$ are shown in figure 46. The conductivity of the latter acid is much lower compared to phosphoric acid in the whole temperature range studied. The disulfonic acid solution has higher conductivities than phosphoric acid at temperatures above 70°C. Comparison of the conductivity data (pH = 1) for two monosulfonic acids having a terminal SF_5 group and a symmetrical disulfonic acid with an ether linkage are illustrated in figure 47. Both mono- and disulfonic acids have higher conductivities than phosphoric acid at high temperatures, the solution of $SF_5CHFCF_2SO_3H$ having the highest conductivity in this group.

CONCLUSIONS

Electrochemical evaluation of a variety of new fluorosulfonic and fluorophosphonic acids have been conducted. The experimental results should be used as guidelines for the synthesise of new acids. The acids tested, in general, have higher oxygen solubilities compared to phosphoric acid. However, long- chain monosulfonic acids such as $C_8F_{17}SO_3H$ are not suitable as fuel cell electrolytes due to their tendency to wet the Teflon structure of the gas diffusion electrodes. Flooding of the fuel cell electrodes has been experienced with several acids having a terminal CF_3 group. Disulfonic acids of the type $(HSO_3)_2(CF_2)_n$ do not wet Teflon. However, the vapor pressures of acids

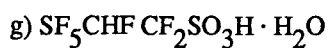
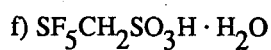
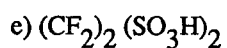
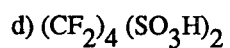
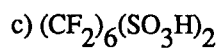
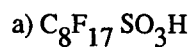
containing only a few CF_2 groups ($n \leq 2$) are high and increasing the fluoroalkyl chain length in order to lower vapor pressure results in a decrease in their water solubilities and conductivities. Thus, even though the acid vapor pressure is low for $n \geq 3$ at temperatures up to 150°C , the low solubility and conductivity limits the useful temperature to less than 100°C . In this homologous series, the $n = 2$ (TFEDSA) acid appeared to have the best properties as a fuel cell electrolyte, although its maximum useful operating temperature is only ca. 100°C .

The best performance from a standard Pt fuel cell cathode was obtained using a saturated aqueous solution of $(\text{CF}_3\text{SO}_2)_2\text{CH}_2$ at room temperature (!). Performance of a room temperature cell using this electrolyte was as much as 70 mV higher than an *optimized* cell using 85% H_3PO_4 at 70°C . However, higher temperature H_3PO_4 cells produce cell voltages comparable to the room temperature $(\text{CF}_3\text{SO}_2)_2\text{CH}_2$ cell, and we found that $(\text{CF}_3\text{SO}_2)_2\text{CH}_2$ could not be used effectively at temperatures above 50°C due to limited solubility. A disulfonic acid containing an ether linkage, $[\text{HSO}_3(\text{CF}_2)_2]_2\text{O}$, showed the highest water solubility of any sulfonic acid we have examined. Short chain mono-sulfonic acids containing a terminal SF_5 group also have high water solubilities, and thus reasonable conductivities at temperatures $\geq 100^\circ\text{C}$. However, in both cases the quantities of acids provided to us were not sufficient to perform an adequate analysis of the oxygen reduction kinetics or fuel cell performance. We recommend that more of these two acids be synthesized for evaluation.

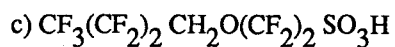
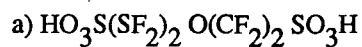
TABLE 1

LIST OF NEW ACIDS RECEIVED FOR TESTING

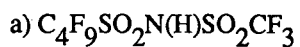
1. Professor G. Gard, Portland State University

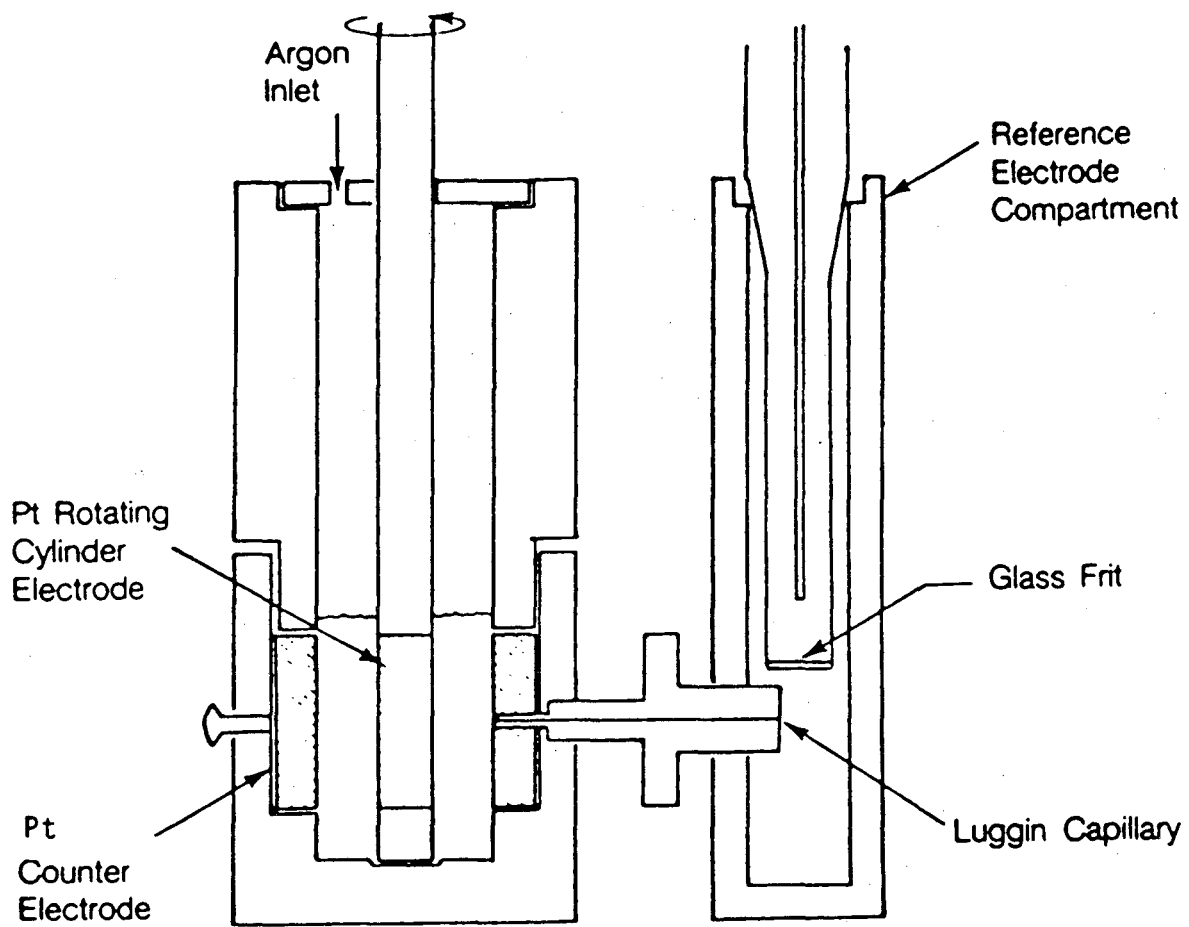


2. Professor J. Shreve, University of Idaho



3. Professor D. Des Marteau, Clemson University





XBL 854-2323

Fig. 1

Rotating Cylinder Electrochemical Cell.

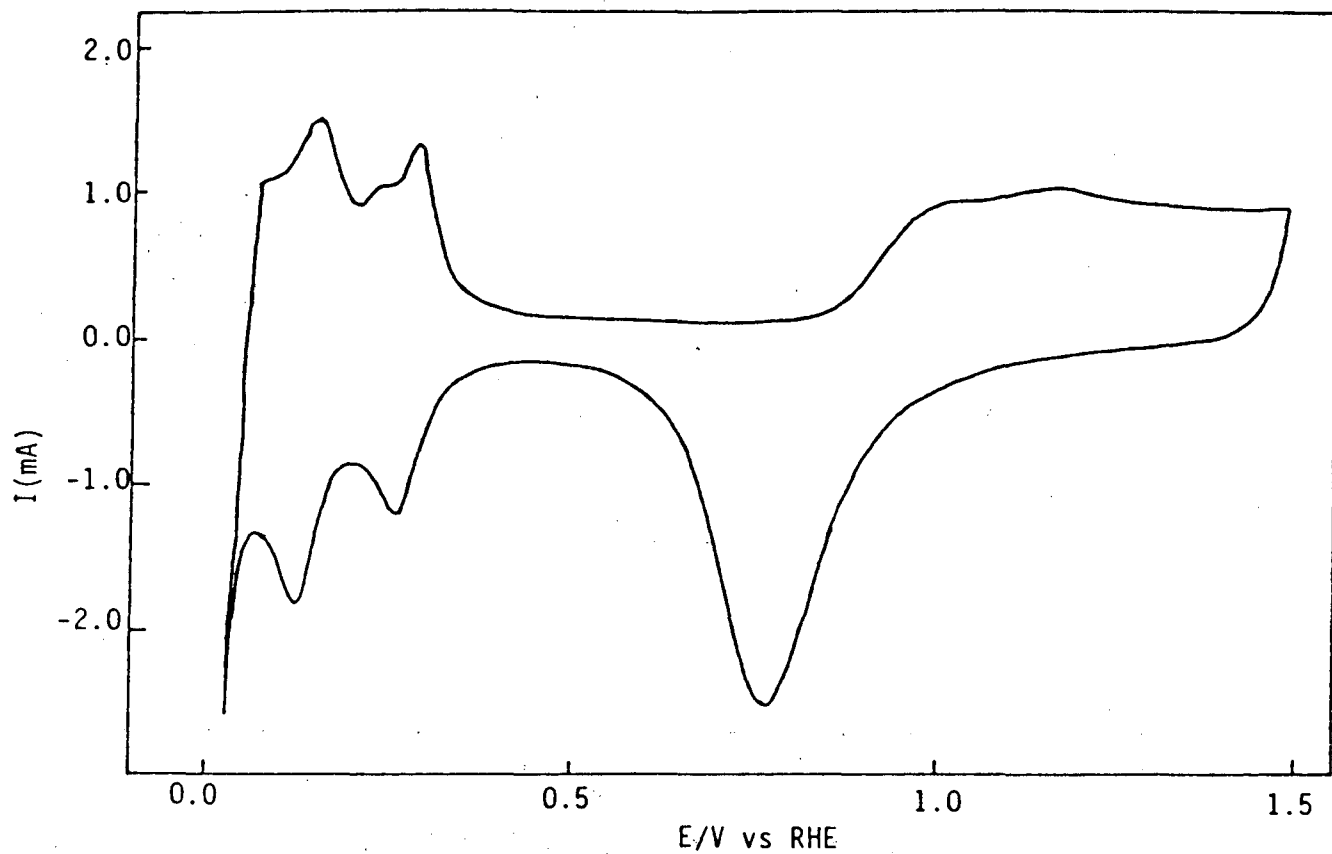


Fig. 2. Cyclic voltammogram of Pt in purified $0.7\text{M H}_3\text{PO}_4$ saturated with N_2 . Scan rate = 100 mV/sec.

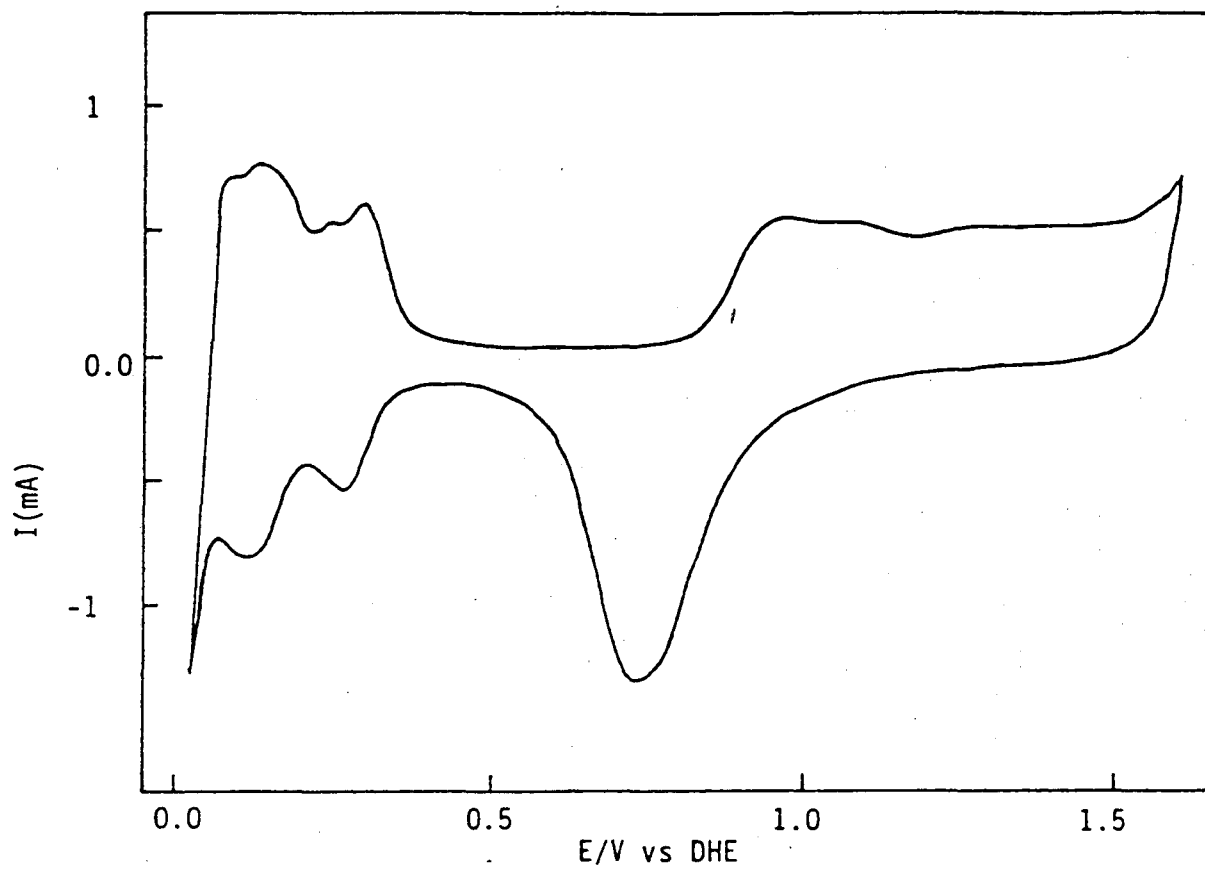


Fig. 3. Cyclic voltammogram of Pt in 0.1M H_2SO_4 saturated with N_2 . Scan rate = 100 mV/sec.

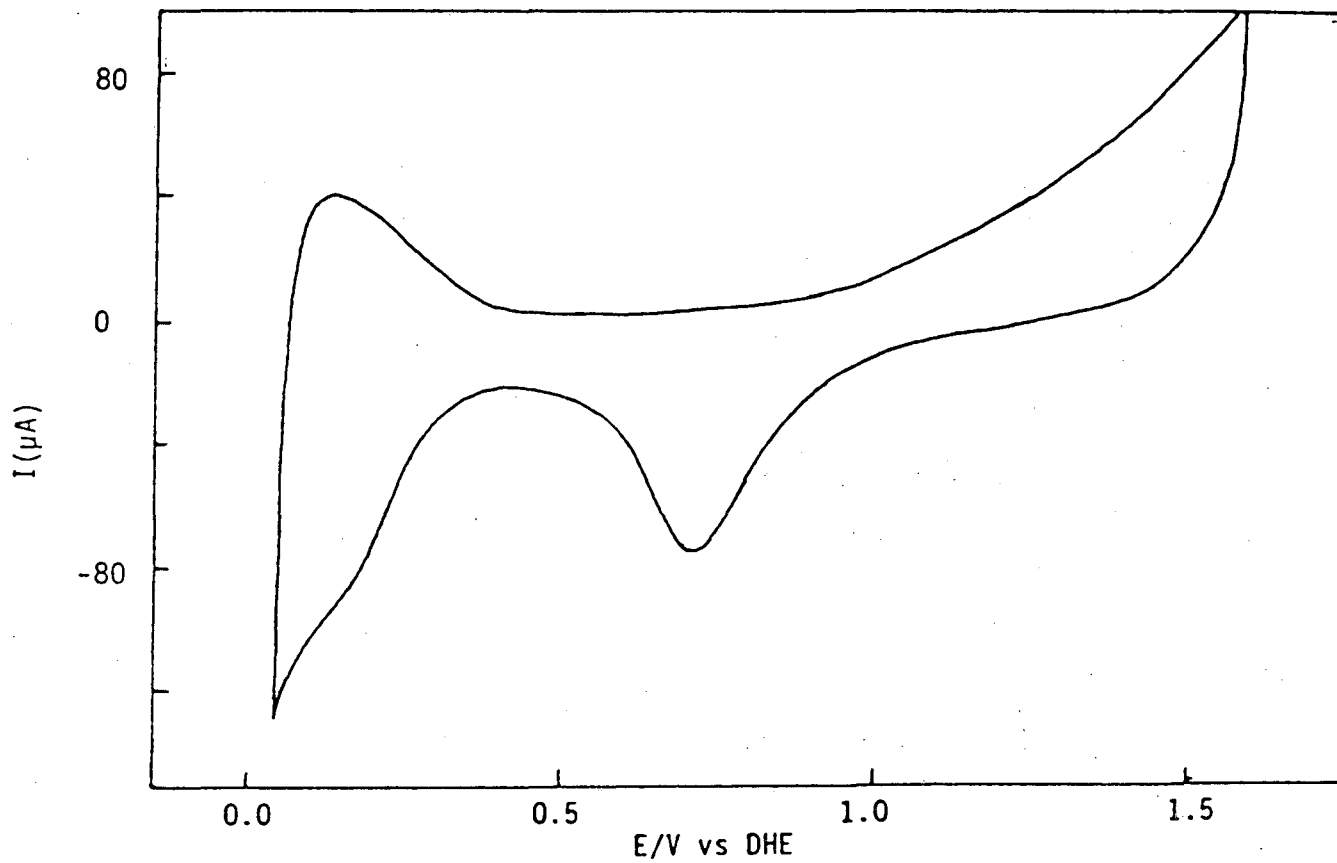


Fig. 4. Cyclic voltammogram of Pt in 0.18M $\text{CF}_3(\text{CF}_2)_2\text{CH}_2\text{O CF}_2\text{CF}_2\text{SO}_3\text{H}$.

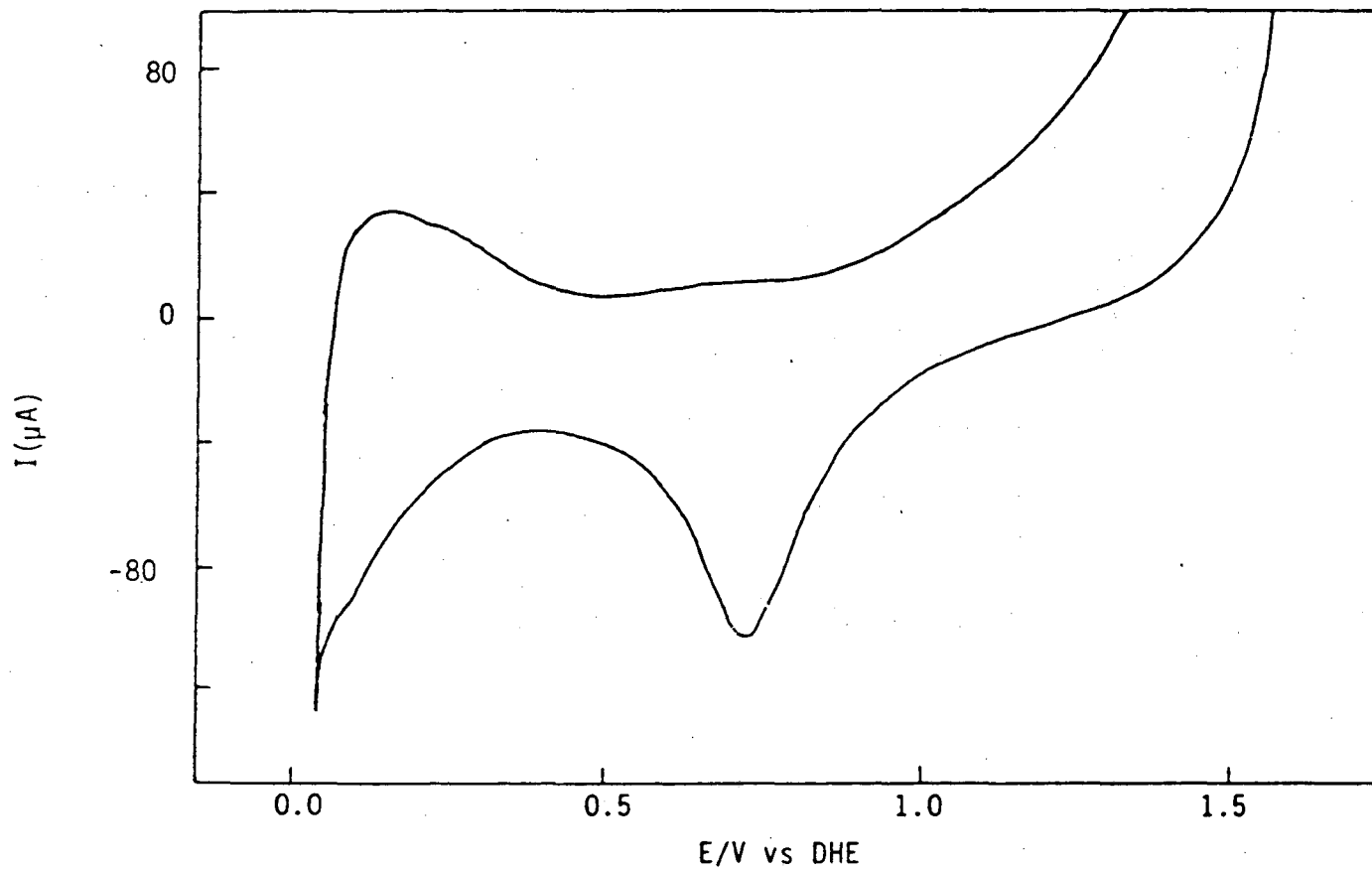


Fig.5 Cyclic voltammogram of Pt in 0.25M $CF_3CH_2O(CF_2)_2SO_3H$.

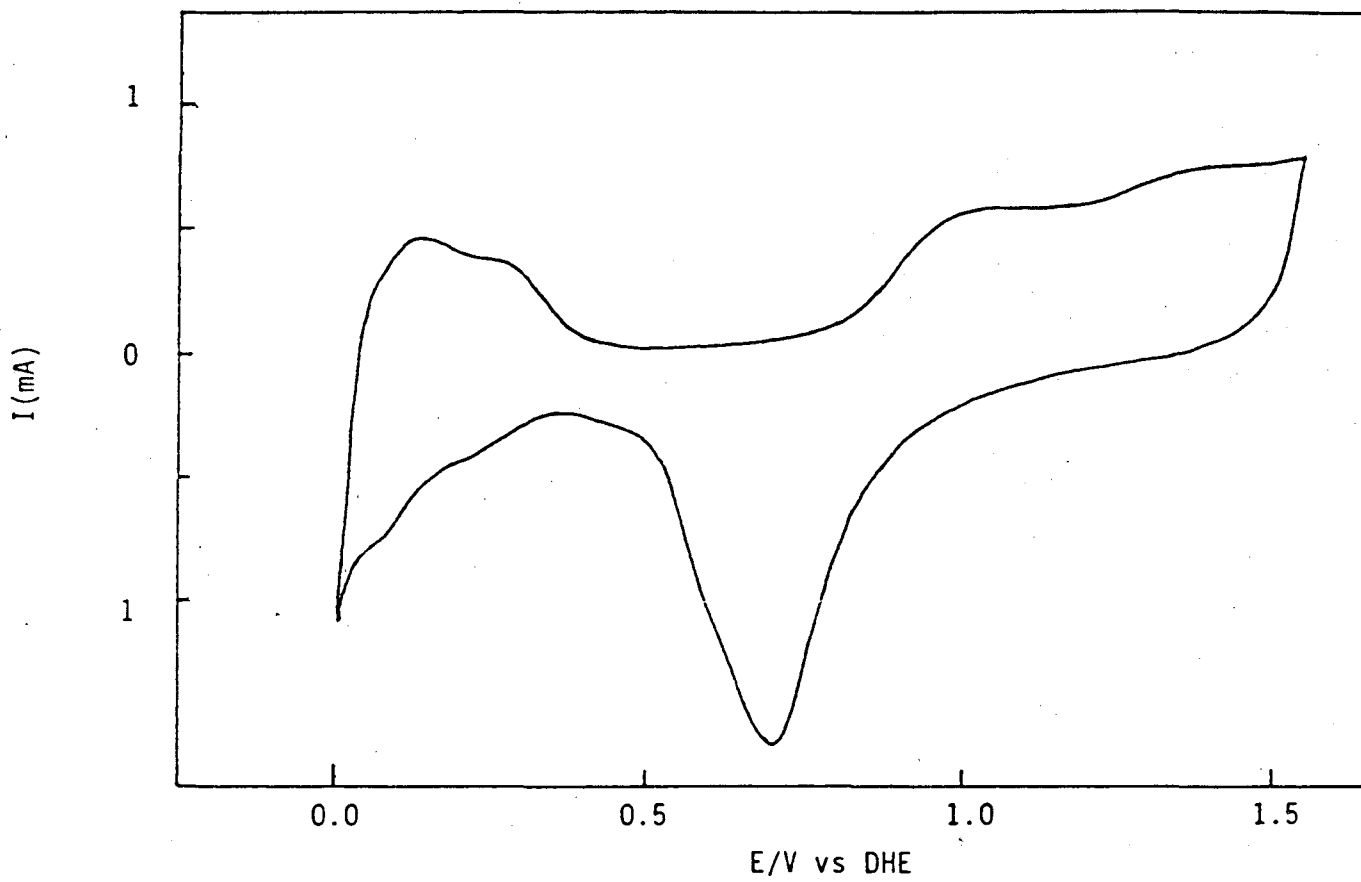


Fig. 6. Cyclic voltammogram of Pt in 0.016M $(\text{CF}_3\text{SO}_2)_2\text{CH}_2$.

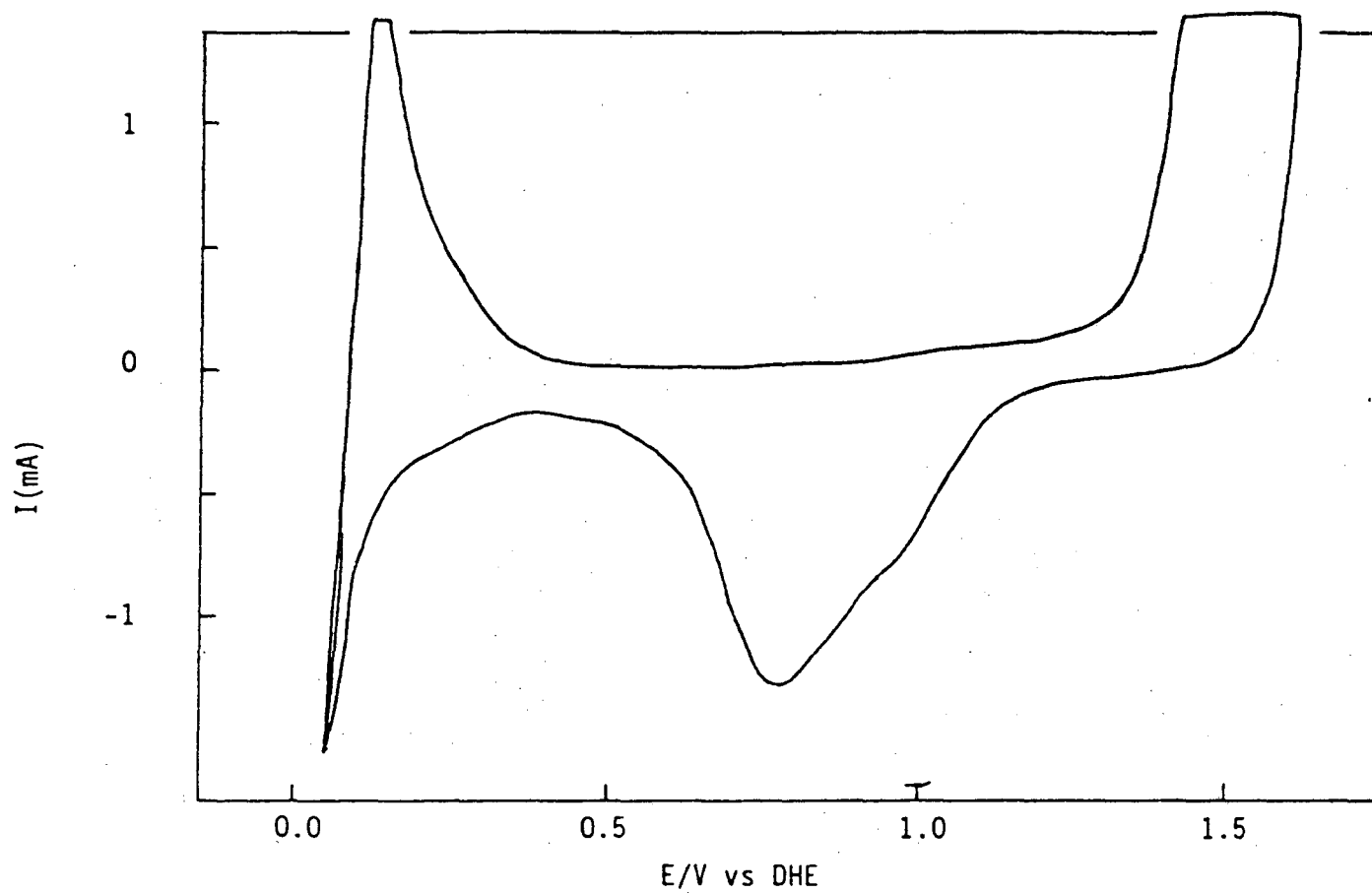


Fig. 7. Cyclic voltammogram of Pt in 0.05M $(\text{HSO}_3(\text{CF}_2)_2)_2\text{O}$.

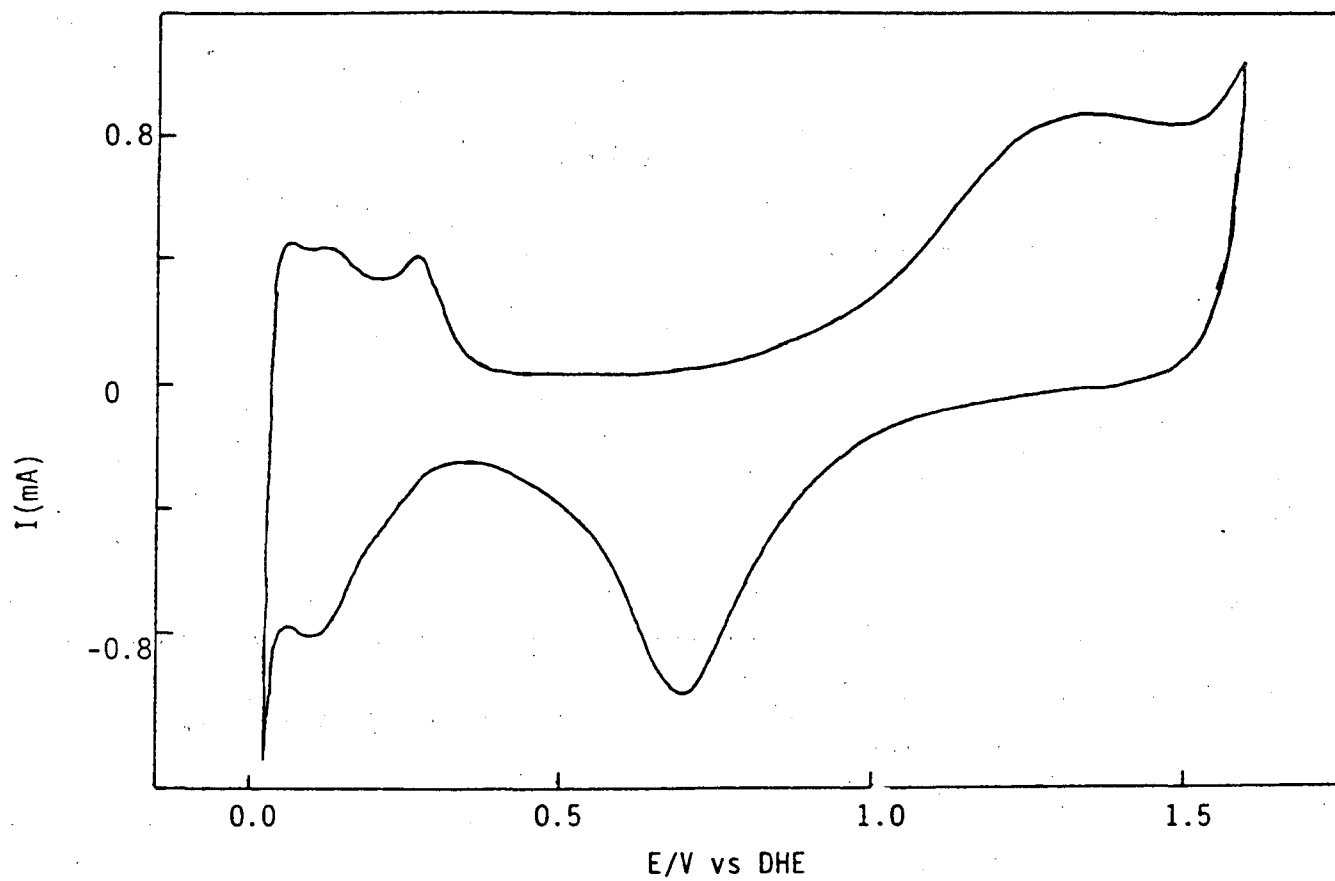


Fig. 8. Cyclic voltammogram of Pt in 0.05M $(\text{HSO}_3(\text{CF}_2)_2)_2\text{O}$ after H_2O_2 treatment.

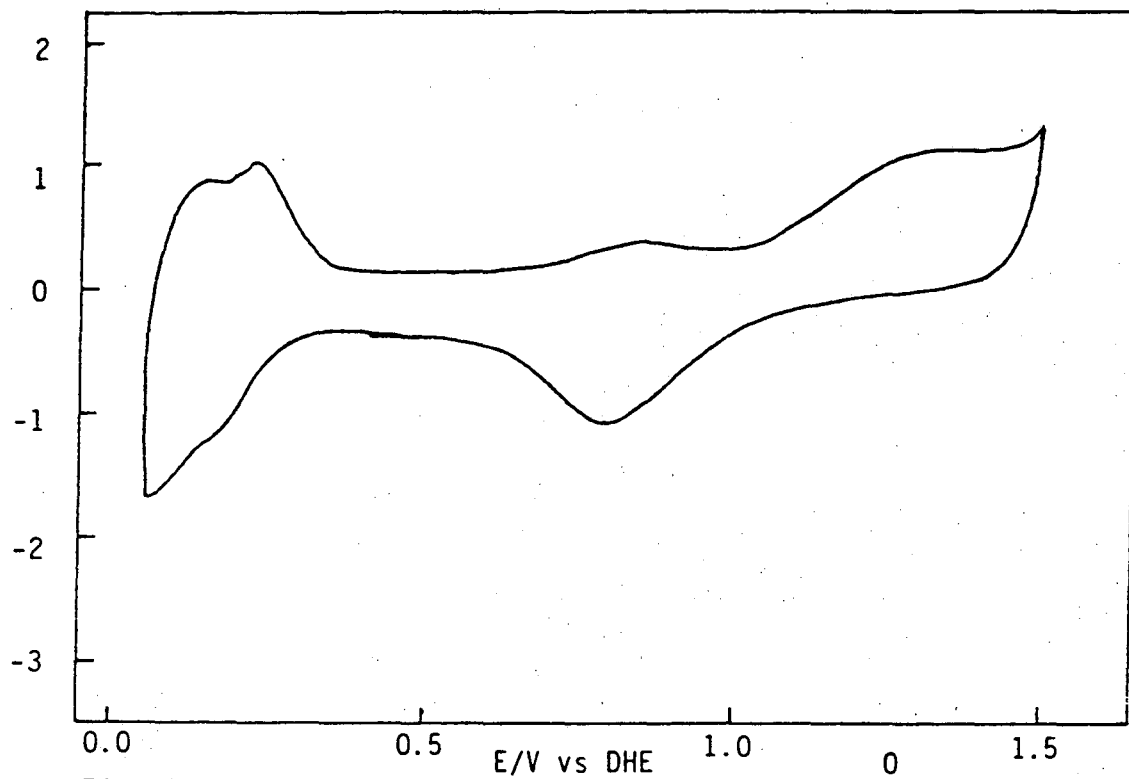


Fig. 9. Cyclic voltammogram of Pt in 0.05M $(\text{HO})_2\text{P}(\text{O})\text{CH}_2(\text{CF}_2)_4\text{CH}_2\text{OH}$.

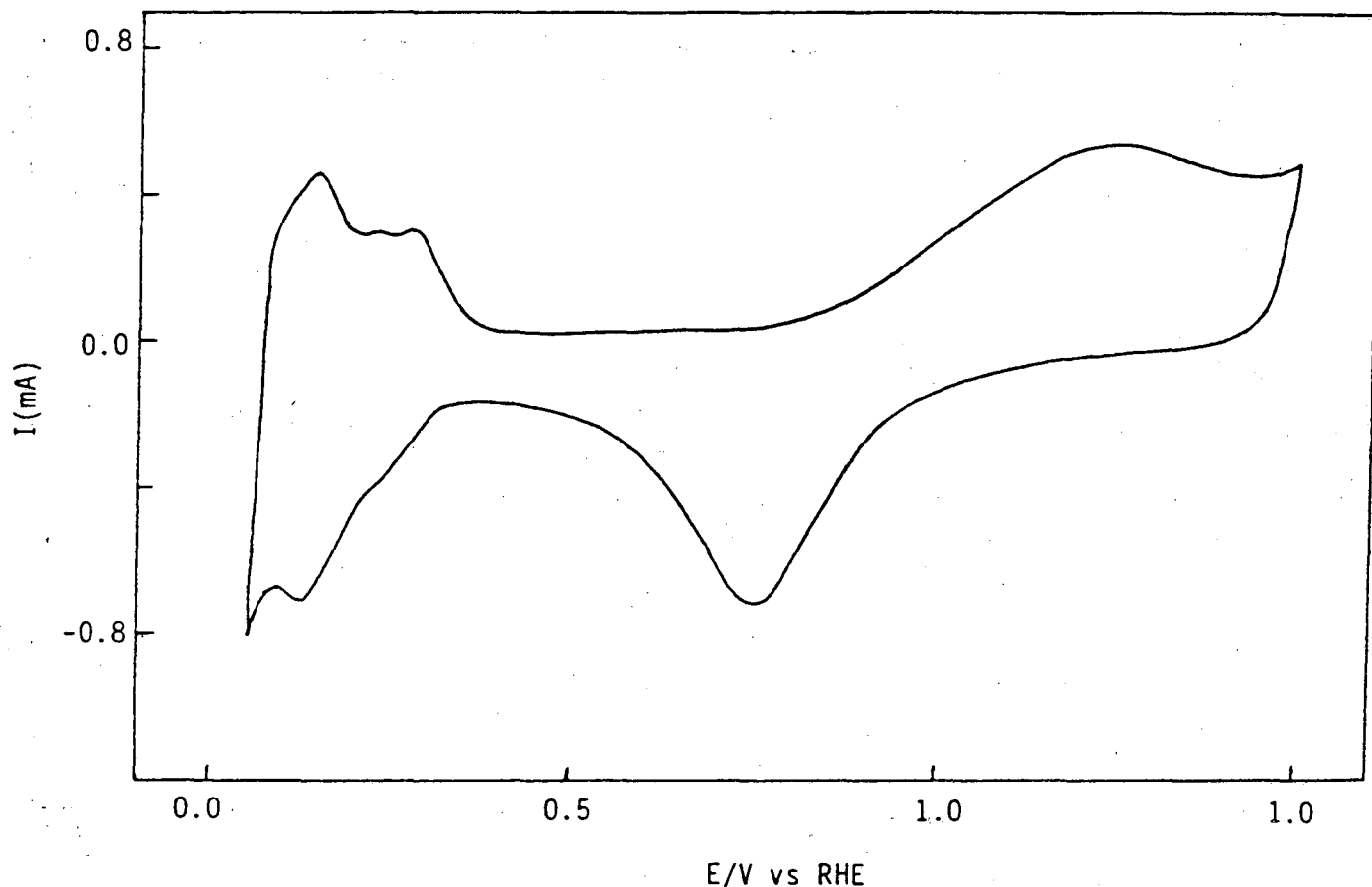


Fig. 10. Cyclic voltammogram of Pt in 0.1M SF₅CH₂SO₃H·H₂O.

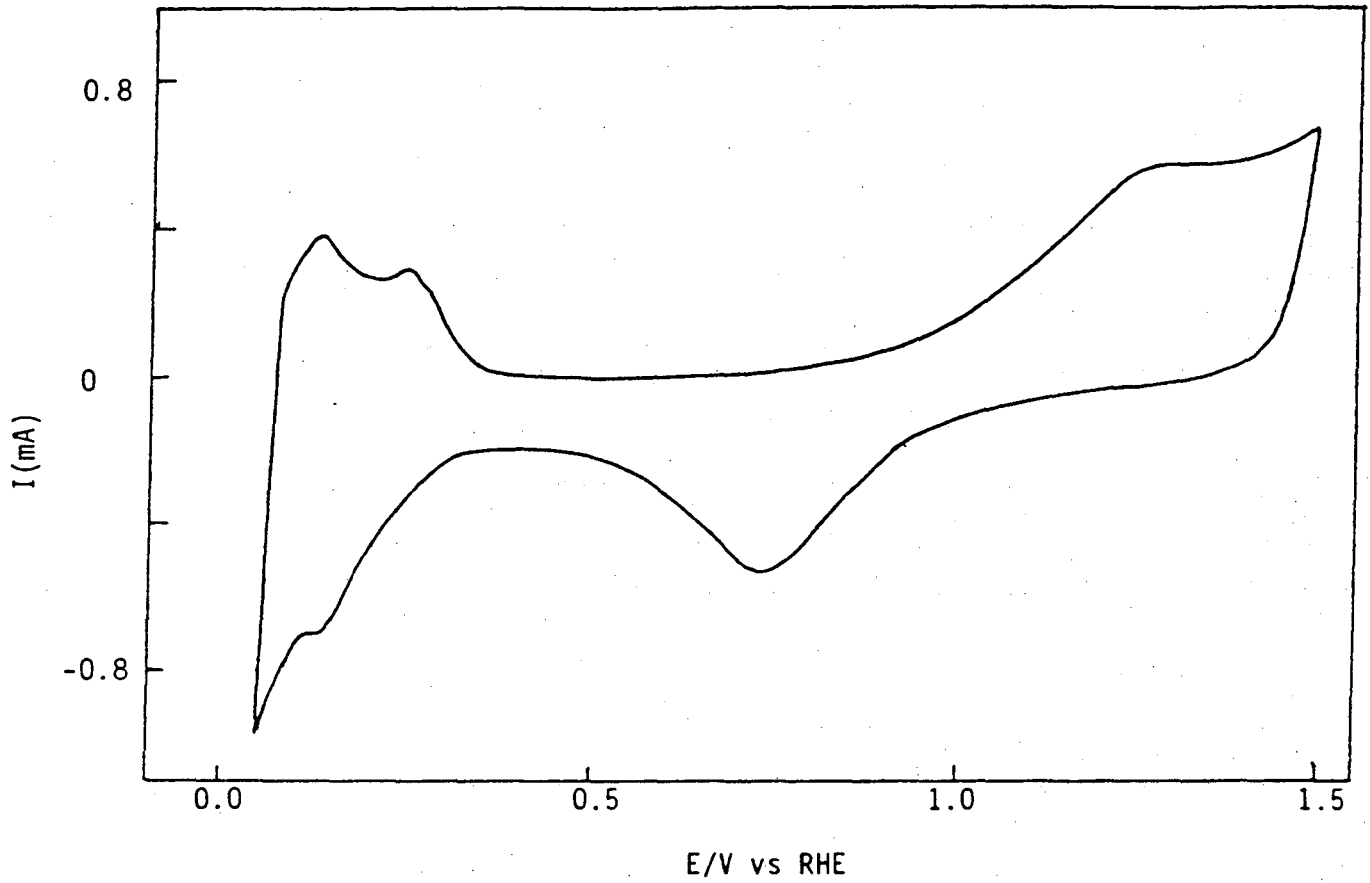


Fig. 11. Cyclic voltammogram of Pt in 0.118M $\text{SF}_5\text{CHFCF}_2\text{SO}_3\text{H} \cdot \text{H}_2\text{O}$.

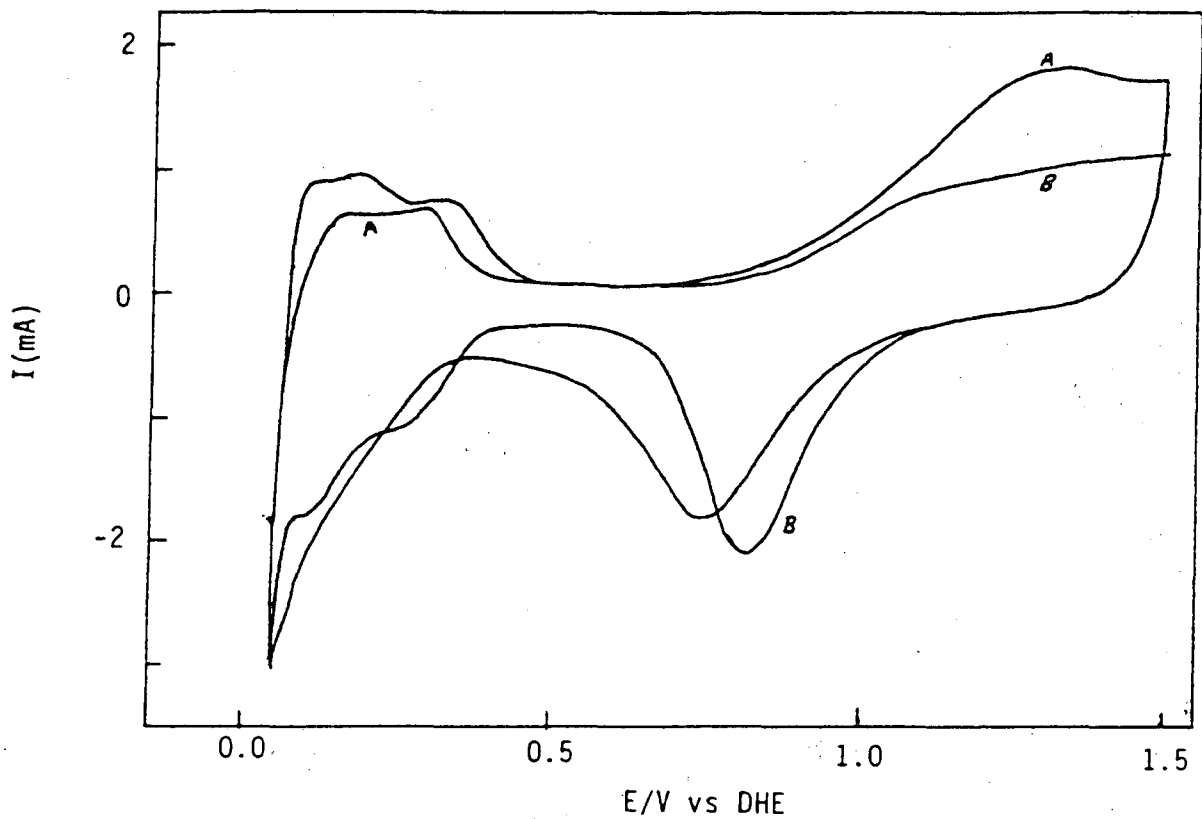


Fig. 12. Cyclic voltammogram of Pt in 0.05M $(CF_2)_6(SO_3H)_2$ (A), and after 48 hours of continuous cycling the electrode potential (B).

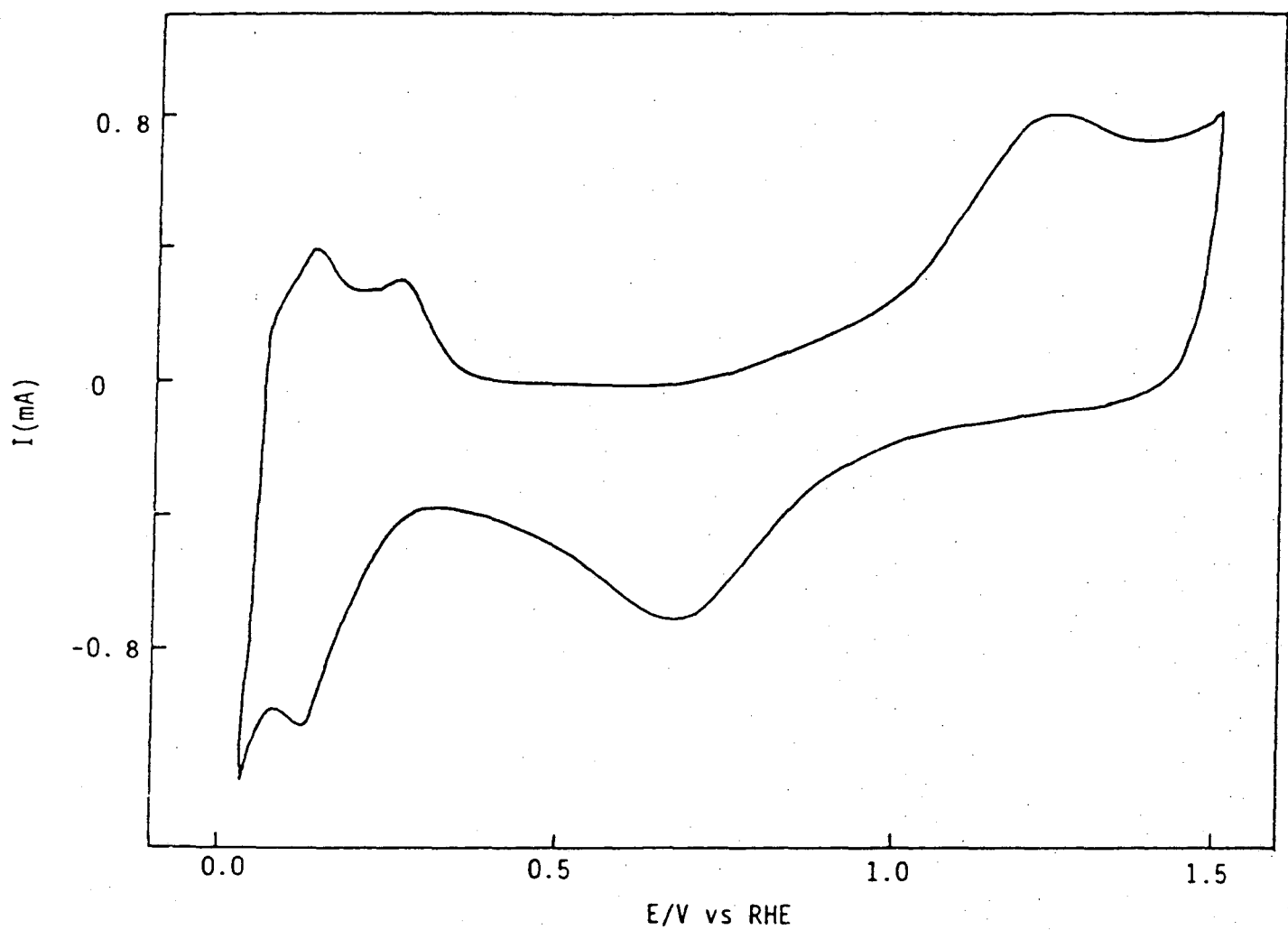


Fig. 13. Cyclic voltammogram of Pt in 0.05M $(CF_2)_6(SO_3H)_2$ after H_2O_2 treatment.

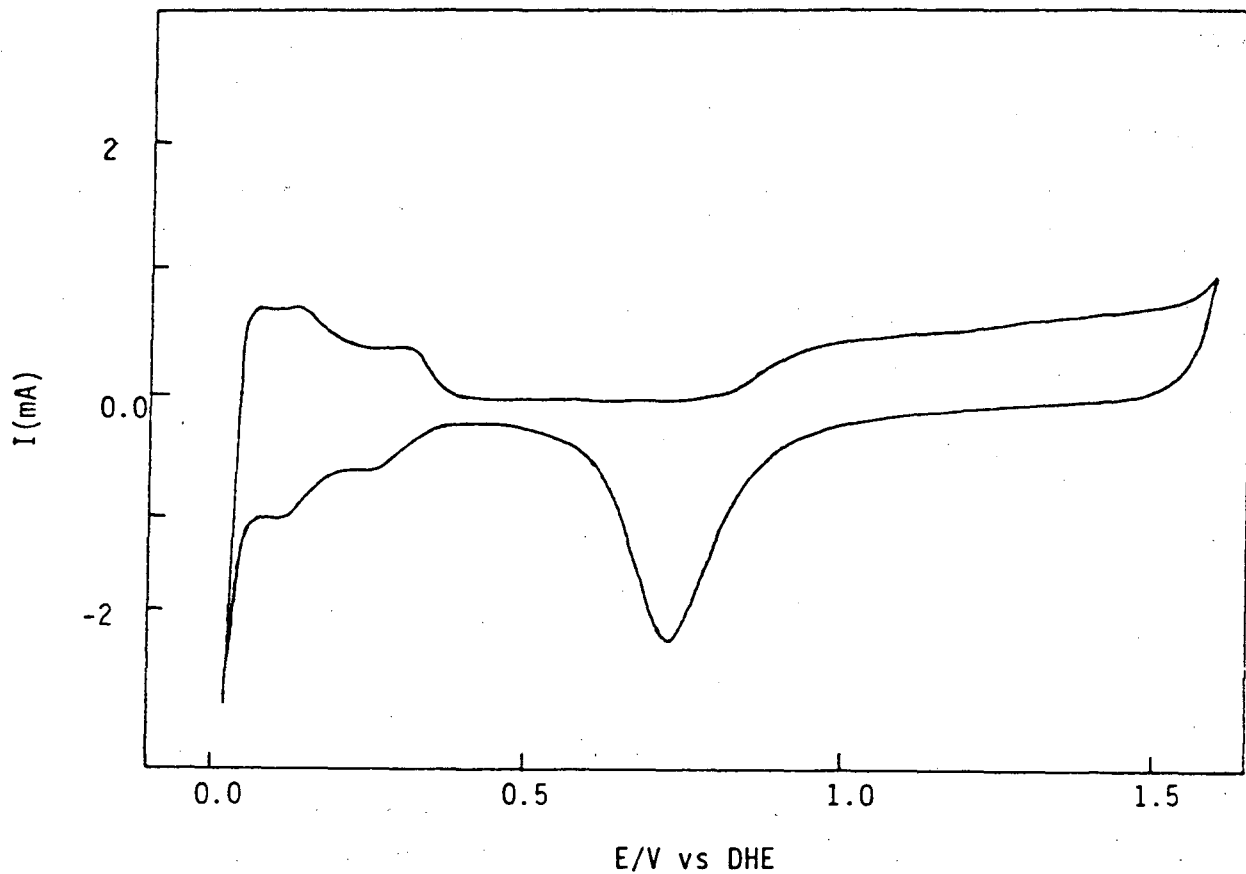


Fig. 14. Cyclic voltammogram of Pt in 0.1M $C_8F_{17}SO_3H$.

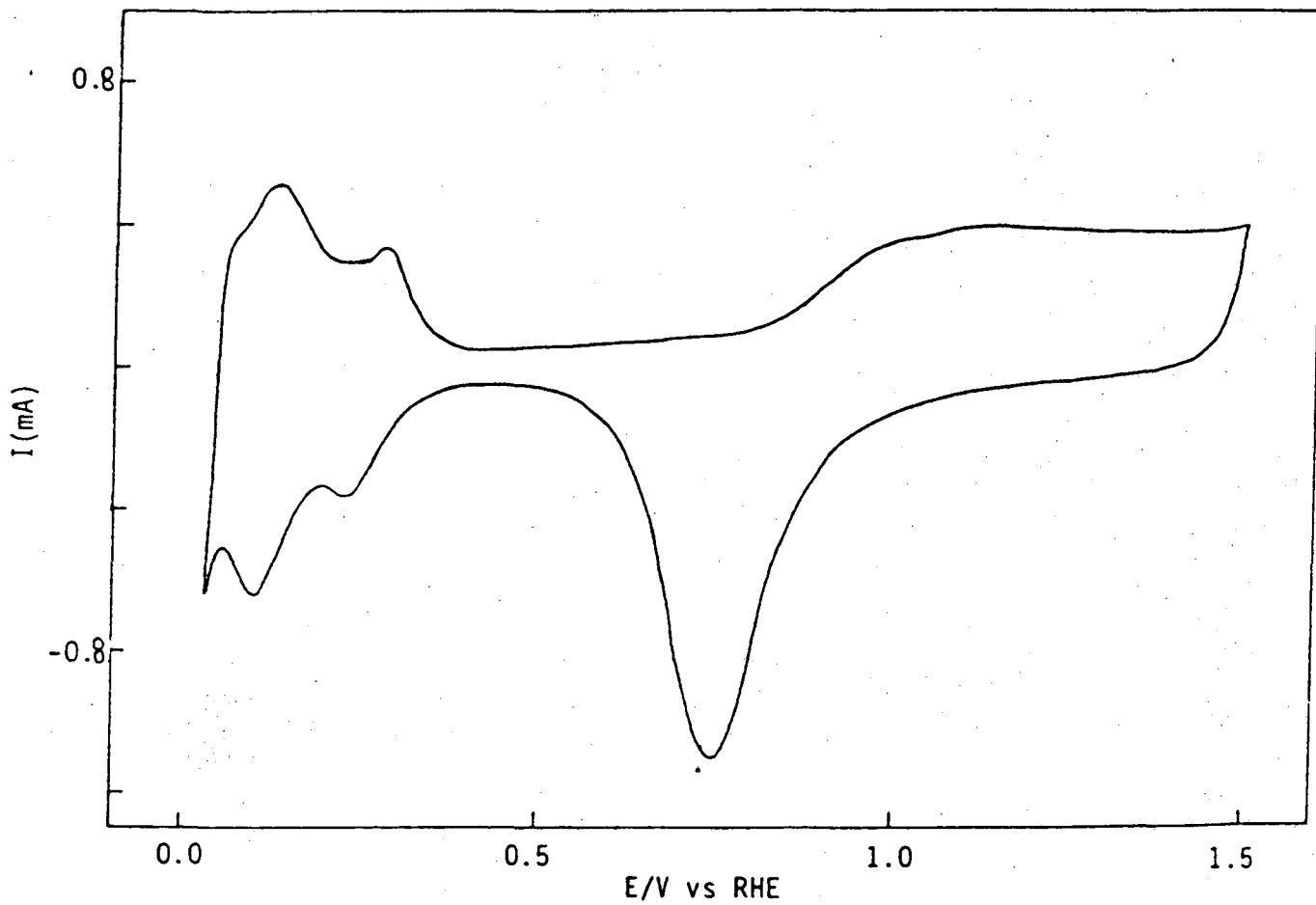


Fig. 15. Cyclic voltammogram of Pt in 0.1M $C_8F_{17}SO_3H$ after H_2O_2 treatment.

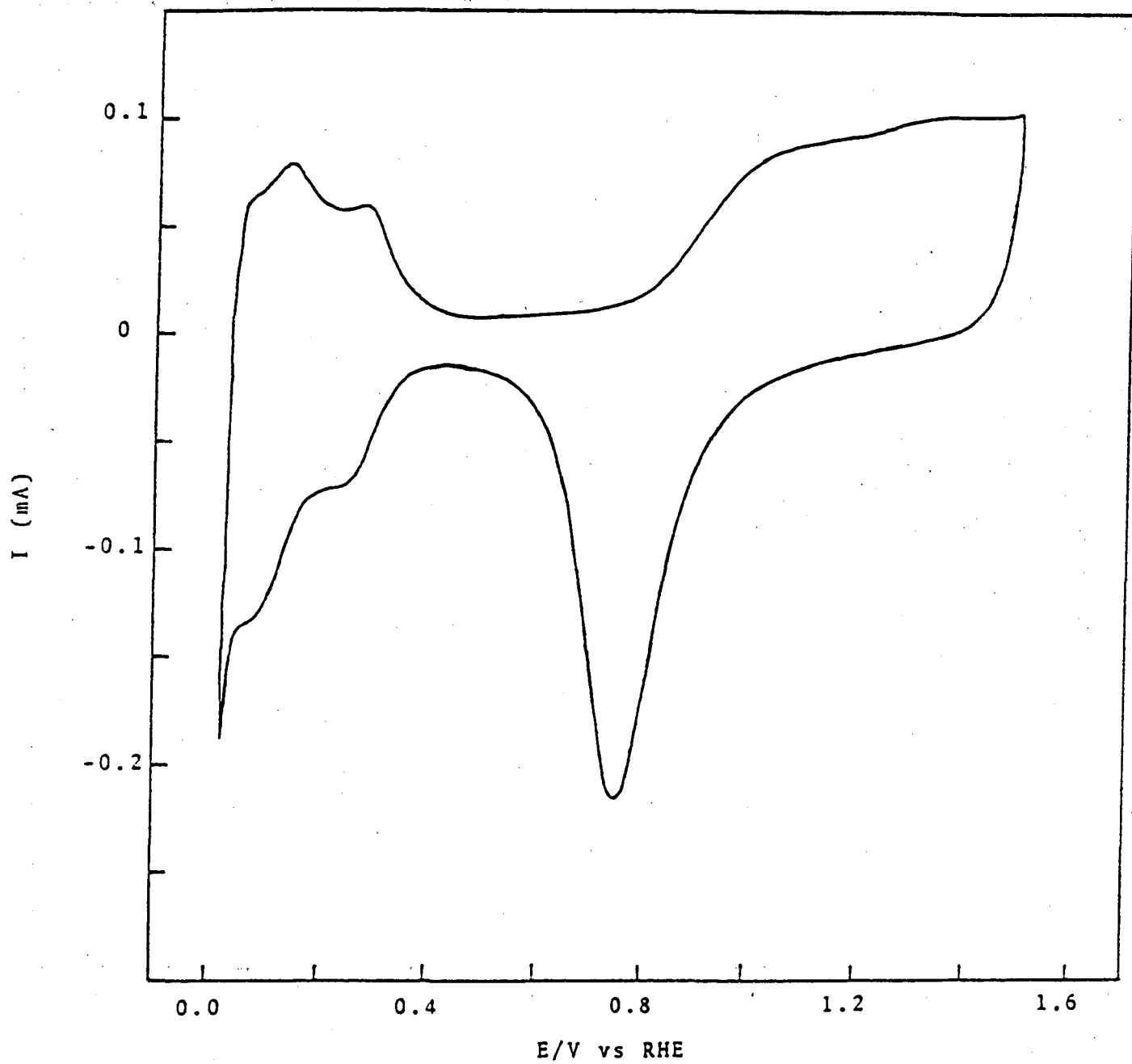


Figure 16 Cyclic voltammogram of Pt in 0.1M $(\text{CF}_2)_4(\text{SO}_3\text{H})_2$ saturated with N_2 before purification.

Scan rate: 100 mV/sec

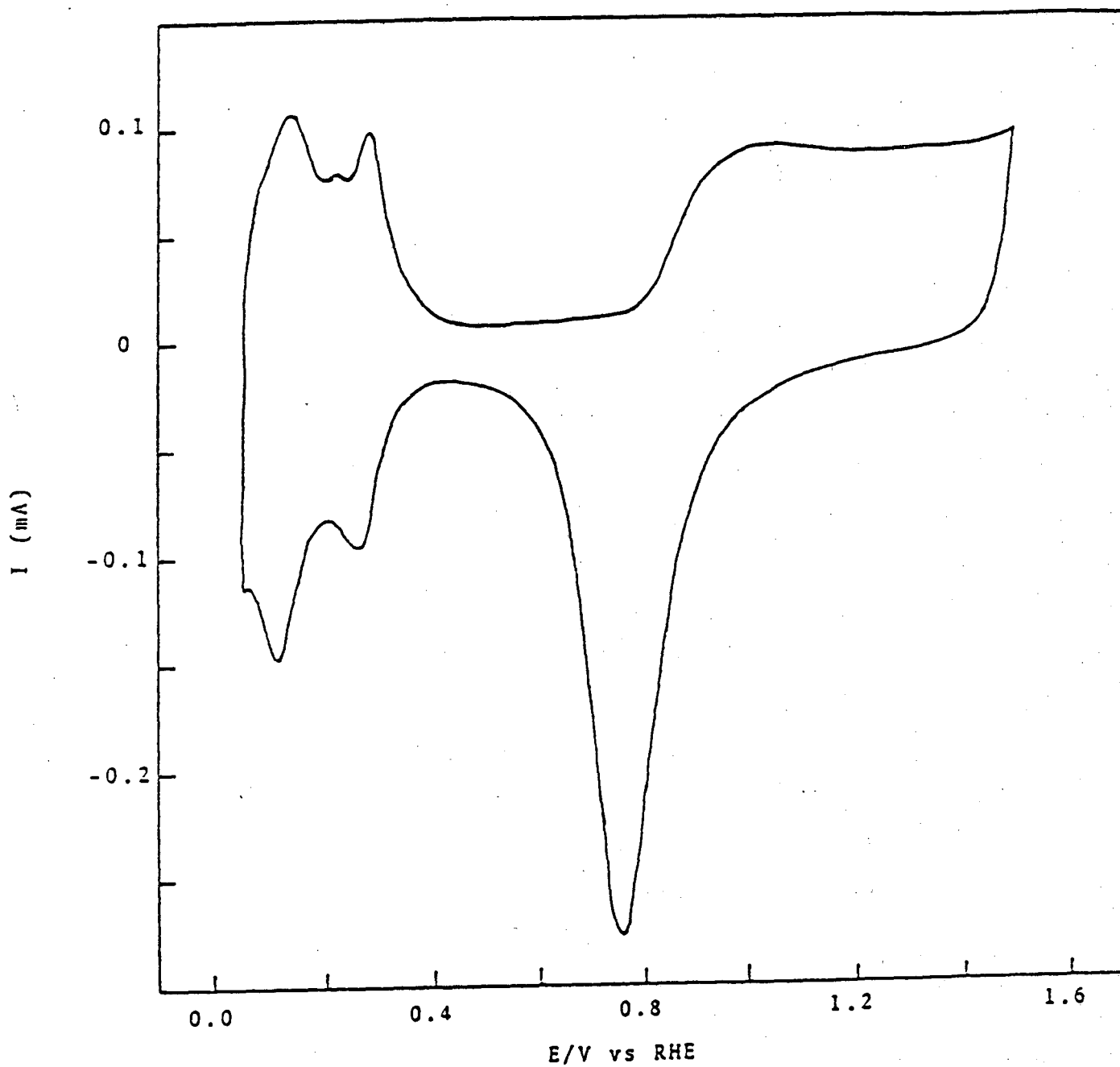


Figure 17 Cyclic voltammogram of Pt in 0.1M $(\text{CF}_2)_4(\text{SO}_3\text{H})_2$ saturated with N_2 after purification.
Scan rate : 100 mV/sec

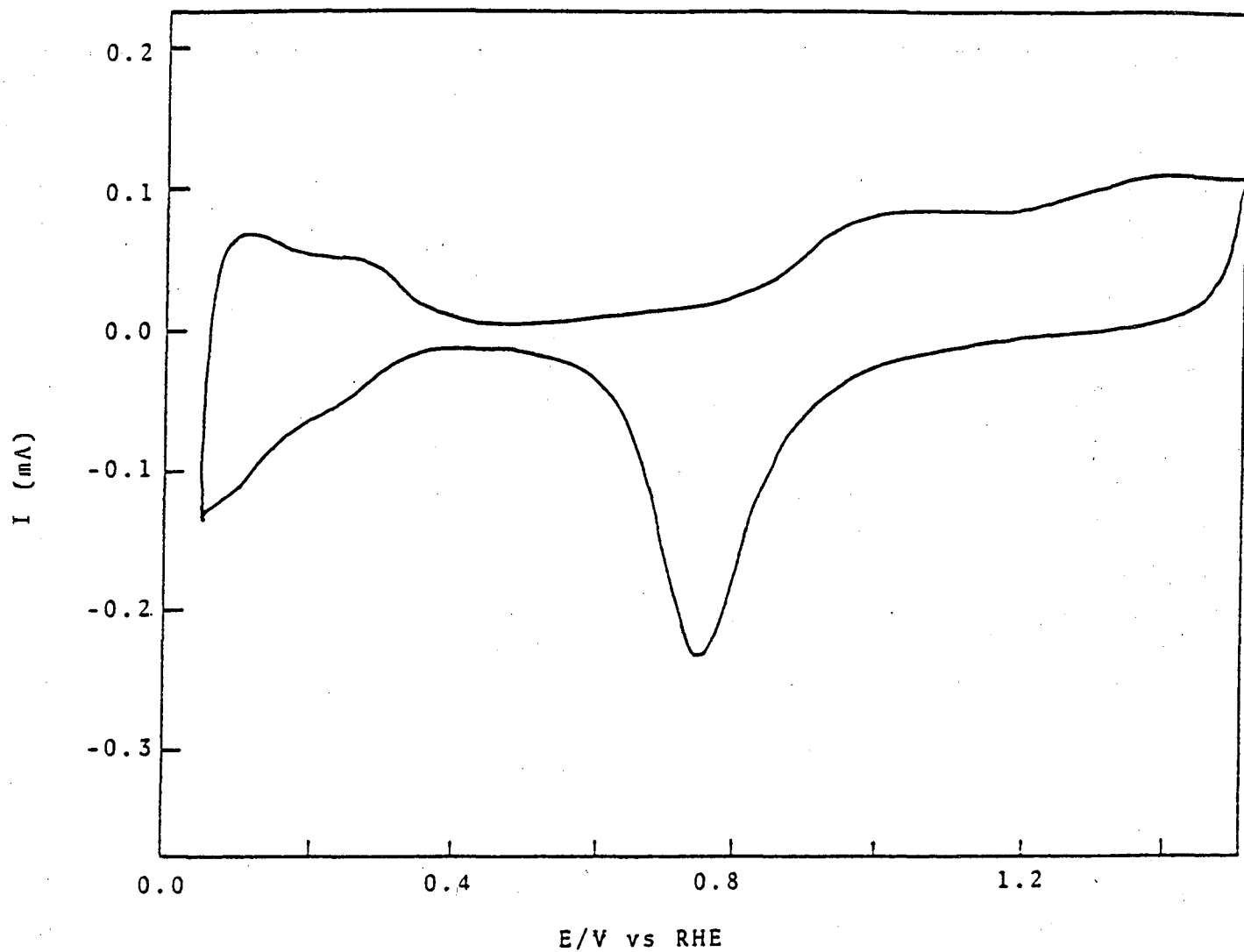


Figure 18 Cyclic voltammogram of Pt in 0.1M $(\text{CF}_3\text{SO}_2)_2\text{CH}_2$ saturated with N_2 before purification.
Scan rate: 100 mV/sec

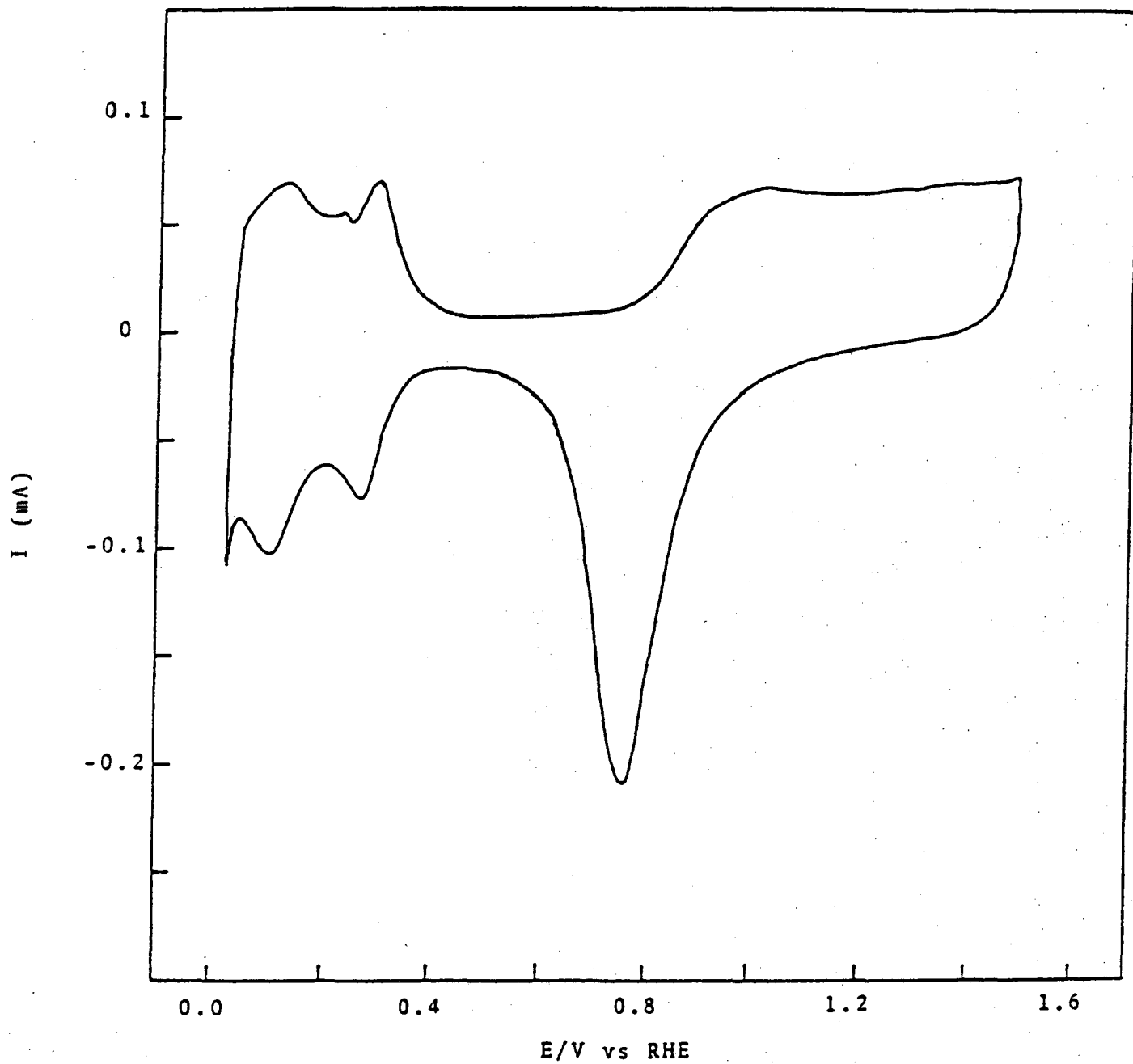


Figure 19 Cyclic voltammogram of Pt in 0.1M $(CF_3SO_2)_2CH_2$ saturated with N_2 after purification.
Scan rate: 100 mV/sec

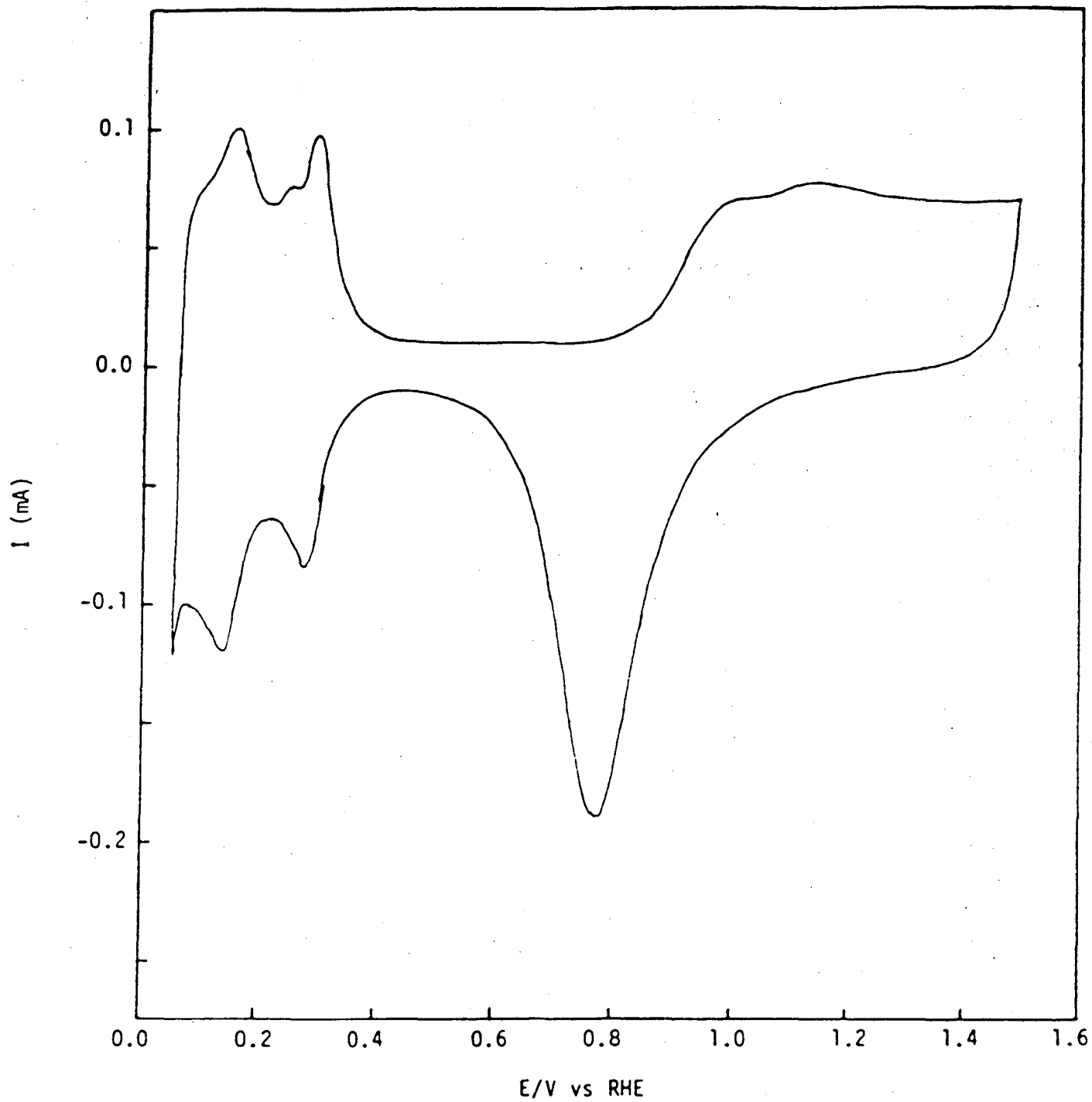


Figure 20 Cyclic voltammogram of Pt in purified 0.1M H_3PO_4 saturated with N_2 .
Scan rate: 100 mV/sec

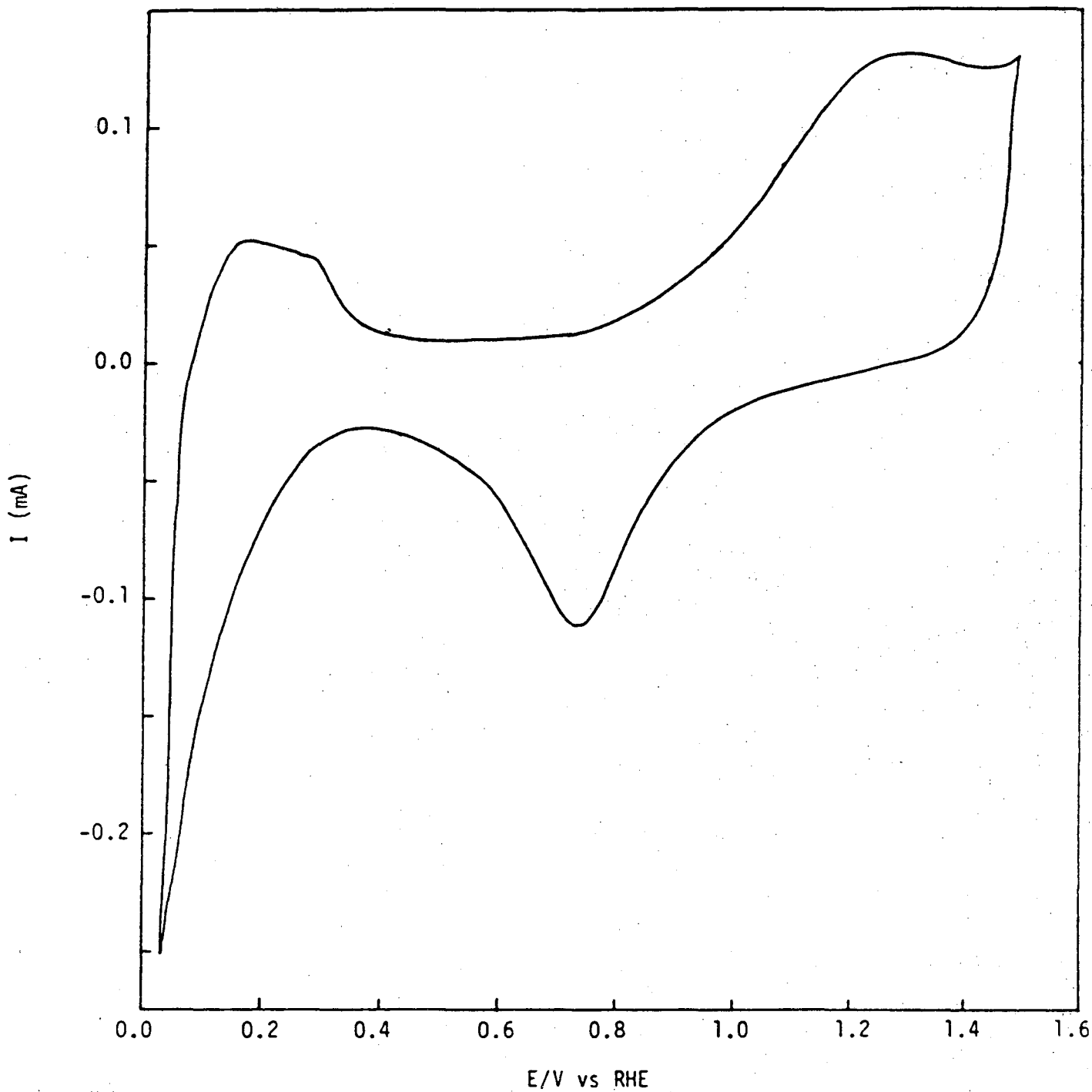


Figure 21 Cyclic voltammogram of Pt in 0.1N $(\text{CF}_2)_6(\text{SO}_3\text{H})_2$ saturated with N_2 before purification. scan rate: 100 mV/sec

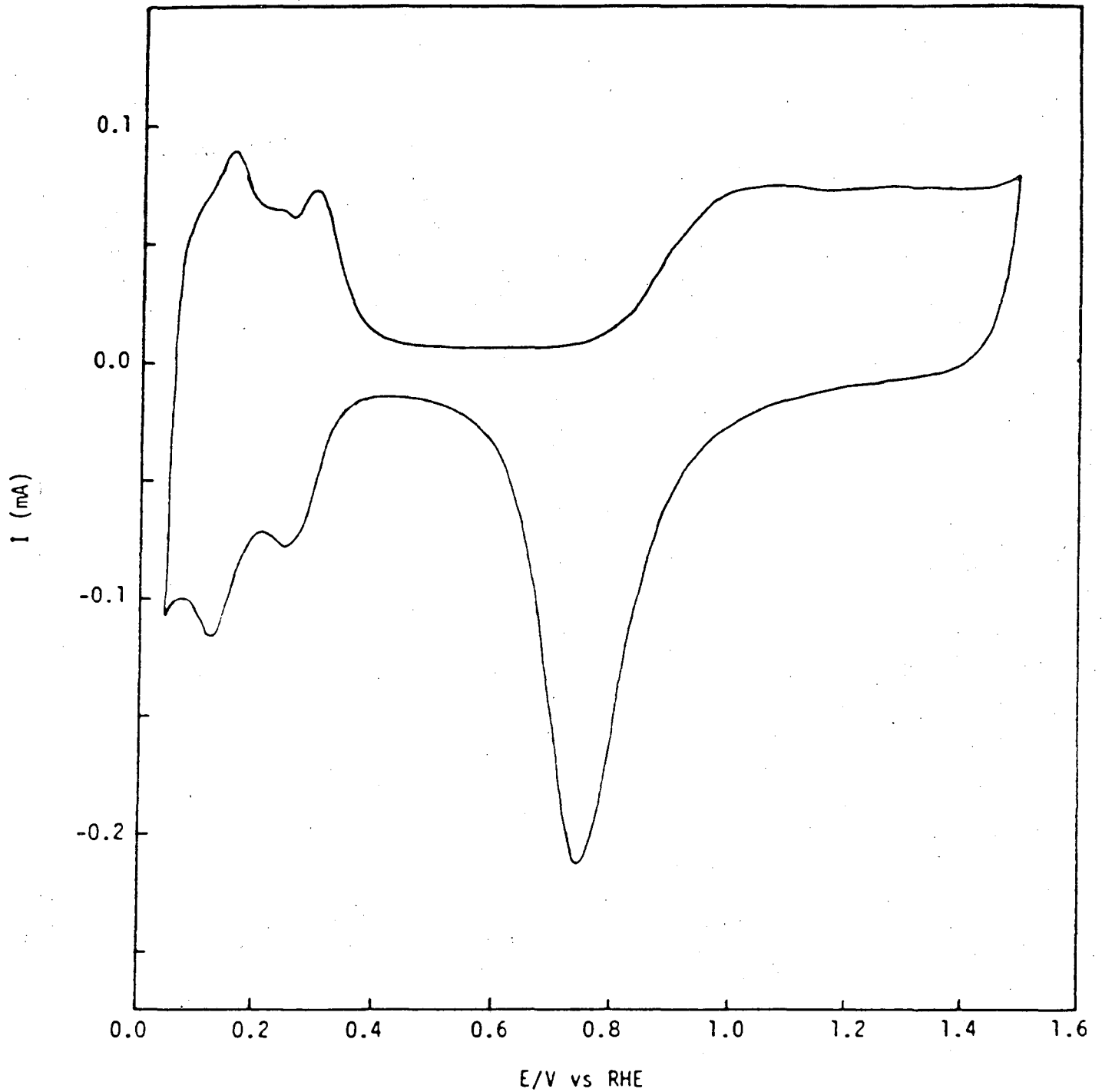


Figure 22 Cyclic voltammogram of Pt in 0.087N $(\text{CF}_2)_6(\text{SO}_3\text{H})_2$ saturated with N_2 after two stages of purification. scan rate: 100 mV/sec

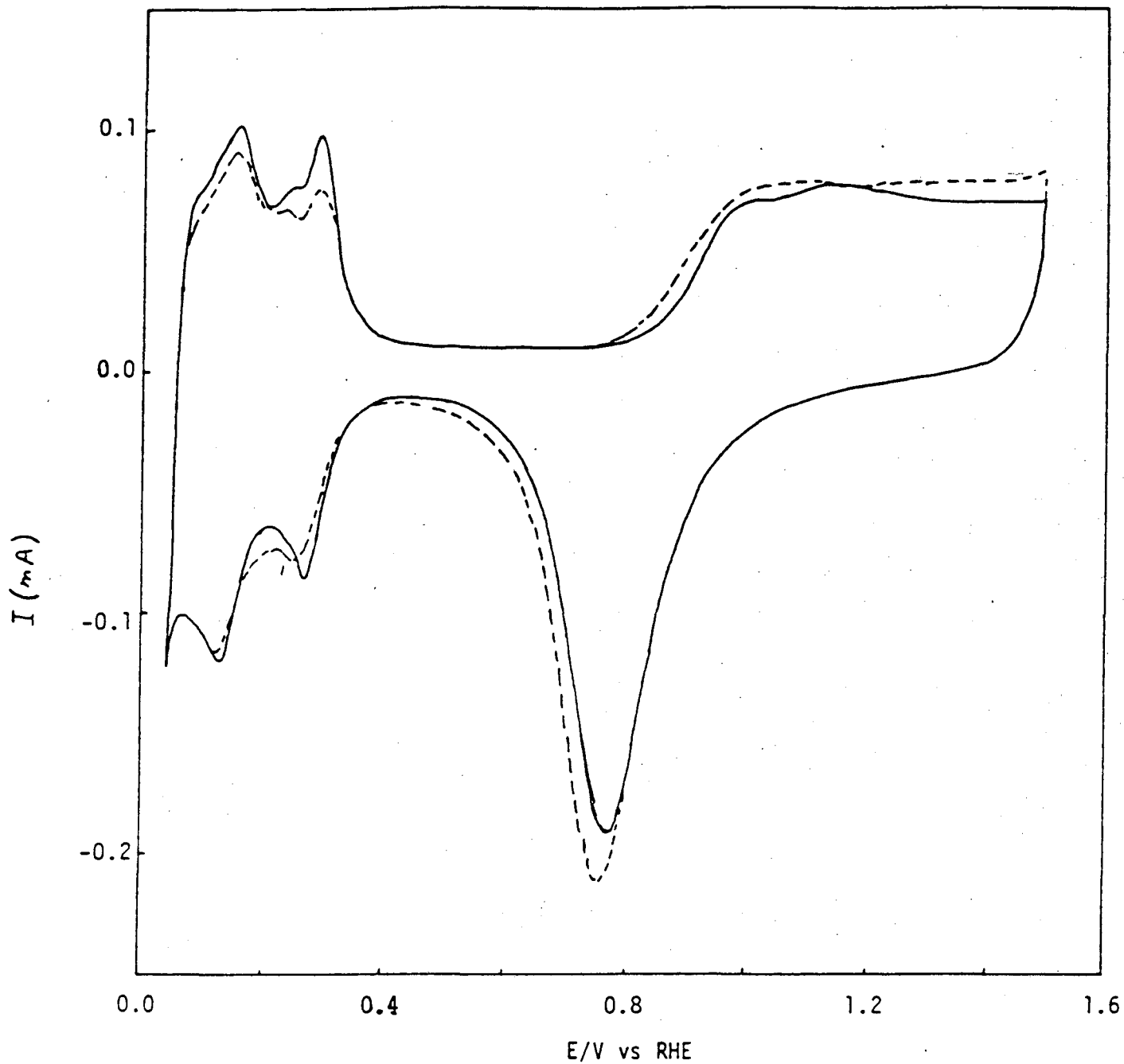


Figure 23 Cyclic voltammograms of Pt in 0.1M H_3PO_4 (—) and 0.087N $(\text{CF}_2)_6(\text{SO}_3\text{H})_2$ (-----) saturated with N_2 . scan rate: 100 mV/sec

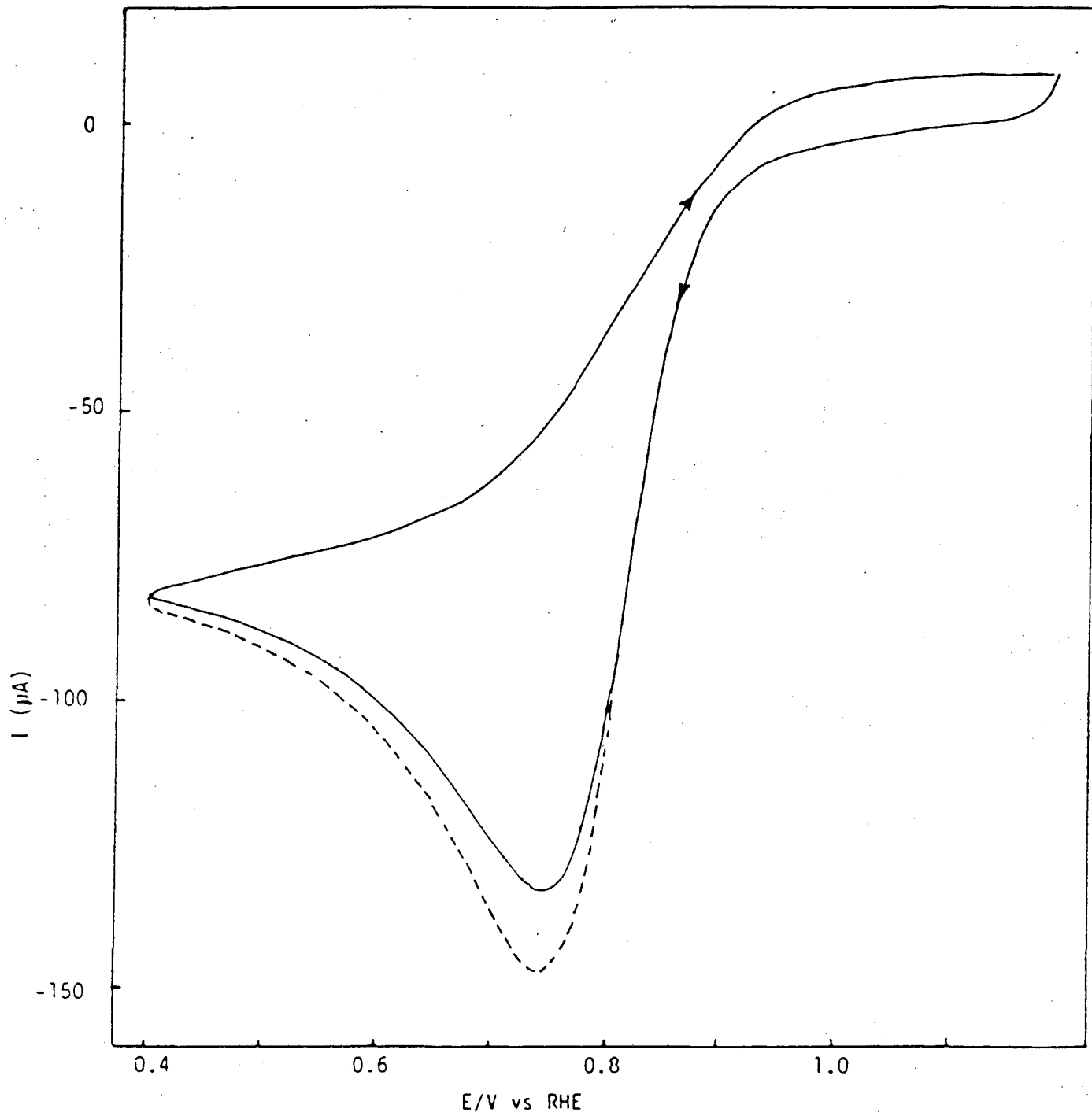


Figure 24 Cyclic voltammogram of Pt in 0.1M H_3PO_4 solution saturated with O_2 .
Scan rate = 10 mV/sec

— first cycle - - - - - third cycle

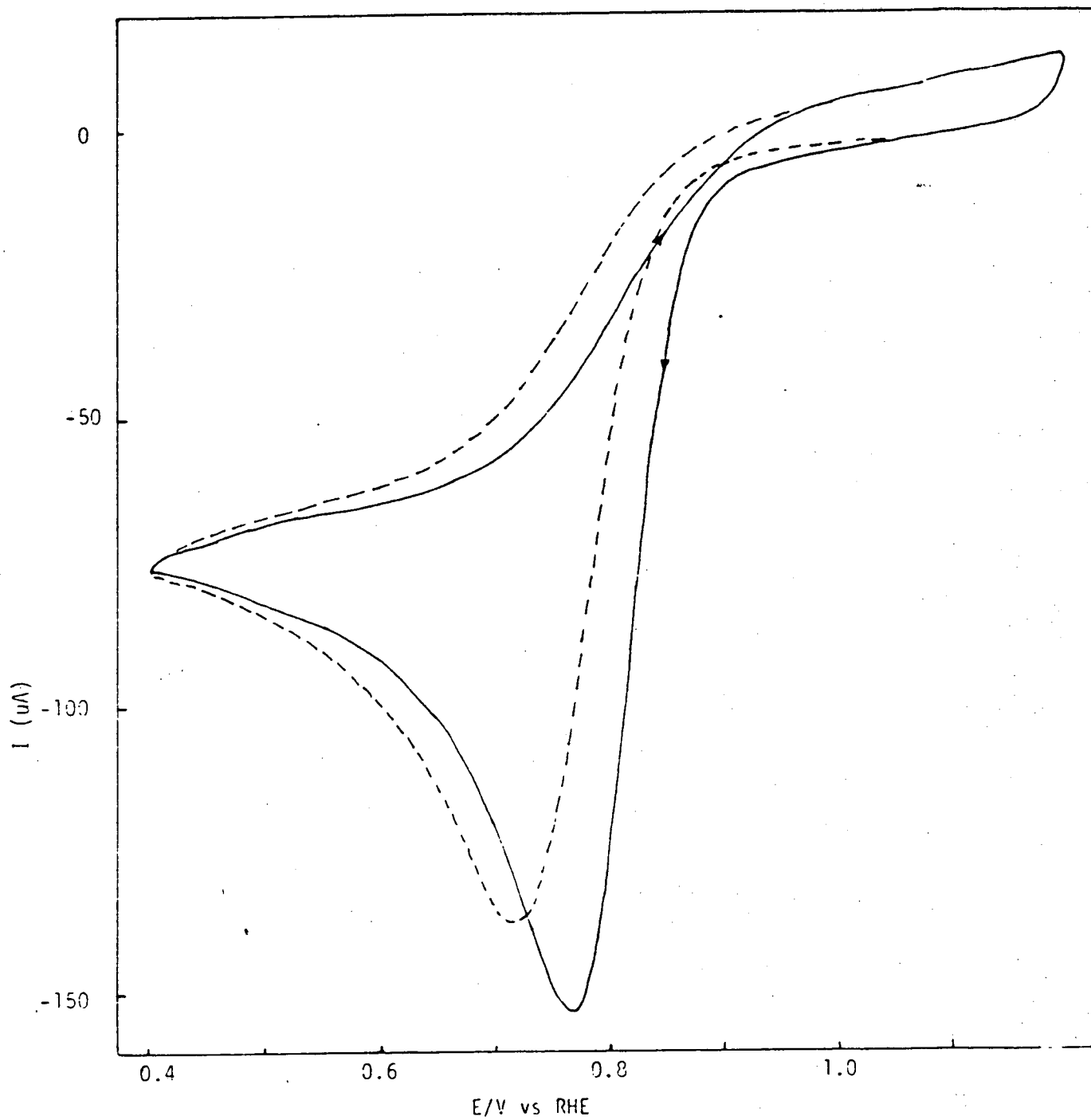


Figure 25 Cyclic voltammogram of Pt in 0.087N $(CF_2)_6(SO_3H)_2$ saturated with O_2 .

scan rate: 10 mV/sec

— first cycle

- - - - - third cycle

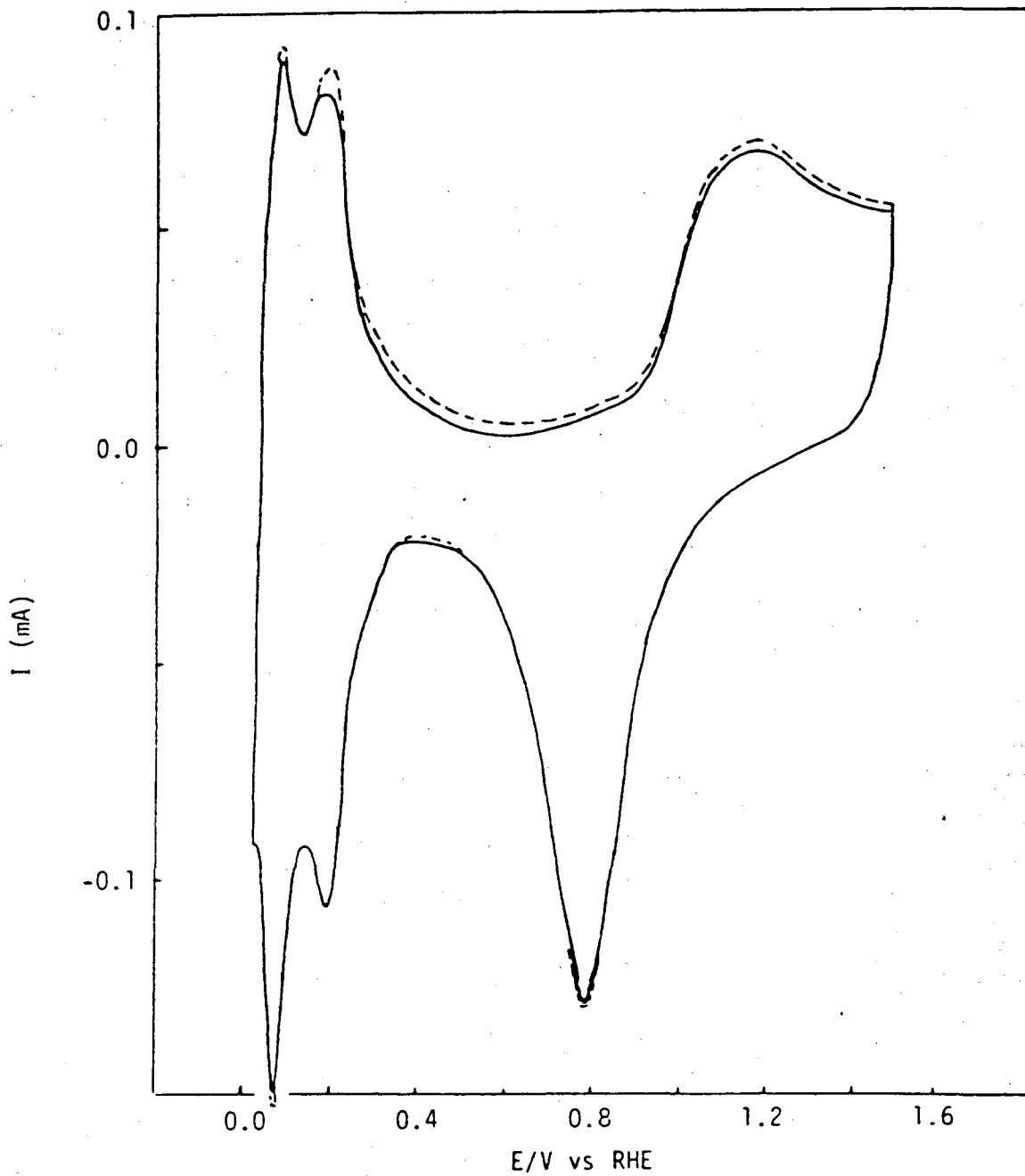


Figure 26 Cyclic voltammograms of Pt in O₂-saturated solutions of 85% H₃PO₄ before (—) and after addition of (CF₂)₆(SO₃H)₂ (-----). Scan rate: 100 mV/sec

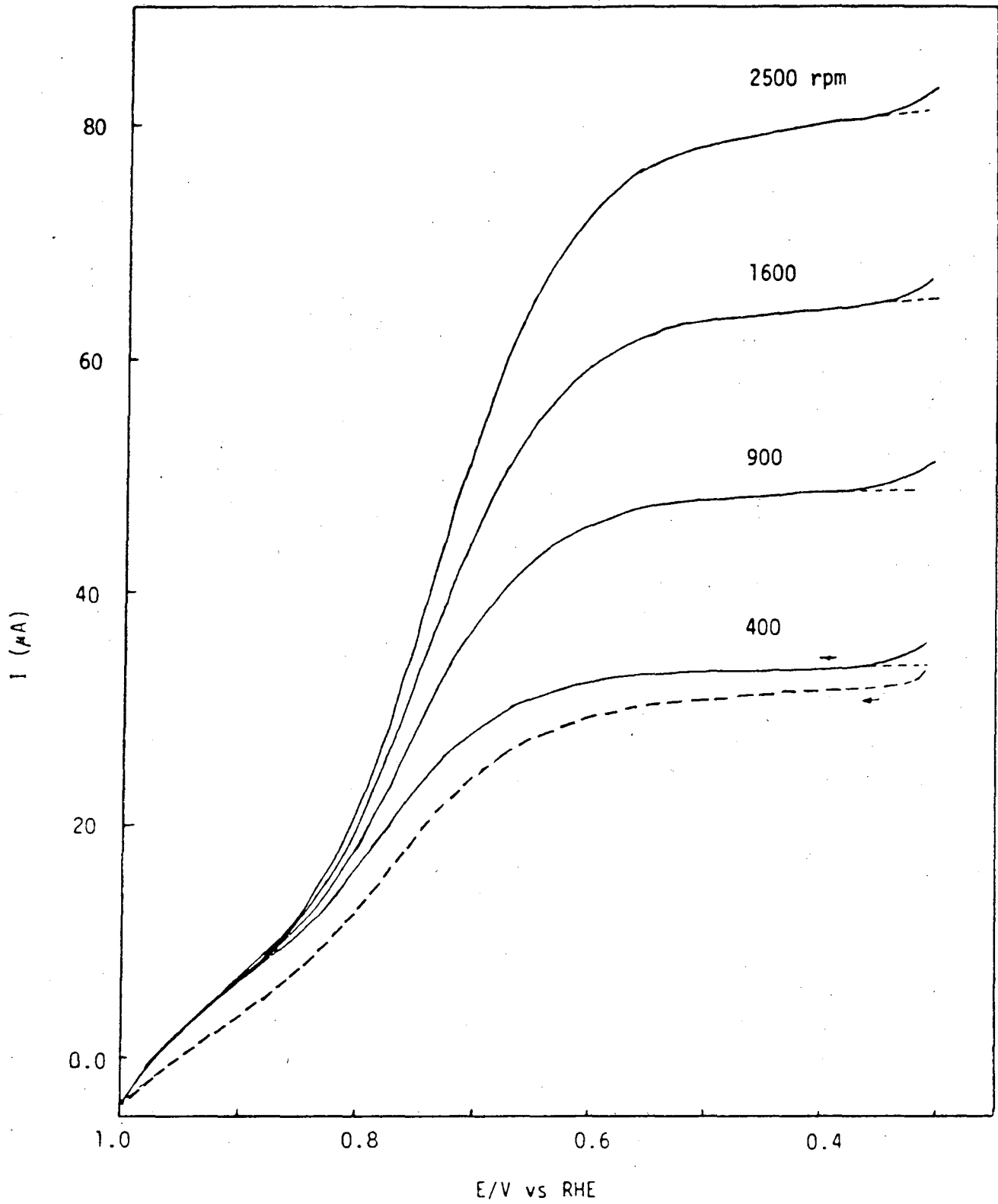


Figure 27 Rotating disk data for O_2 reduction on Pt in 85% H_3PO_4 .

scan rate: 10 mV/sec

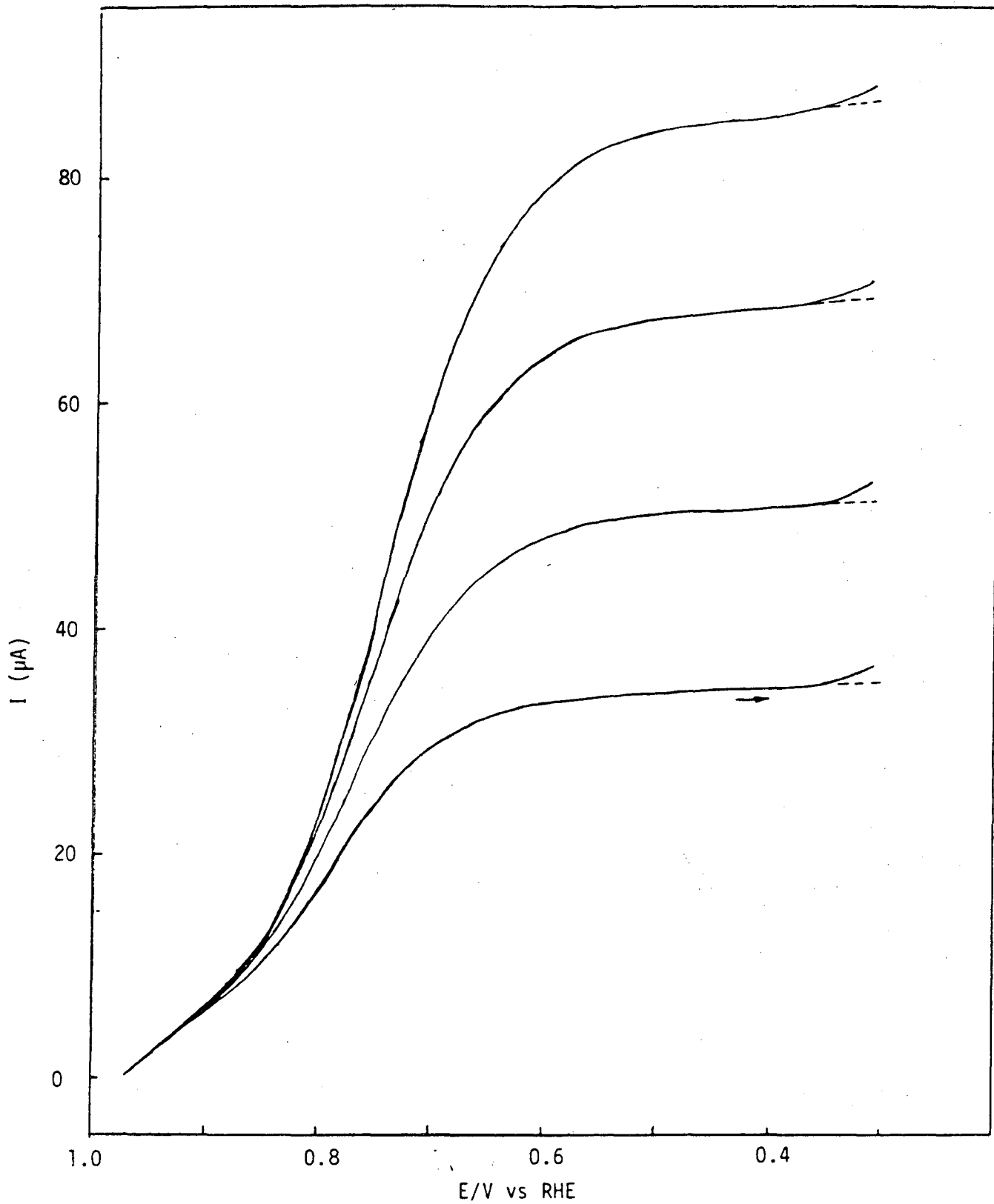


Figure 28 Rotating disk data for O_2 reduction on Pt in 85% H_3PO_4 solution containing 0.45% $(\text{CF}_2)_6(\text{SO}_3\text{H})_2$. Scan rate : 10 mV/sec.

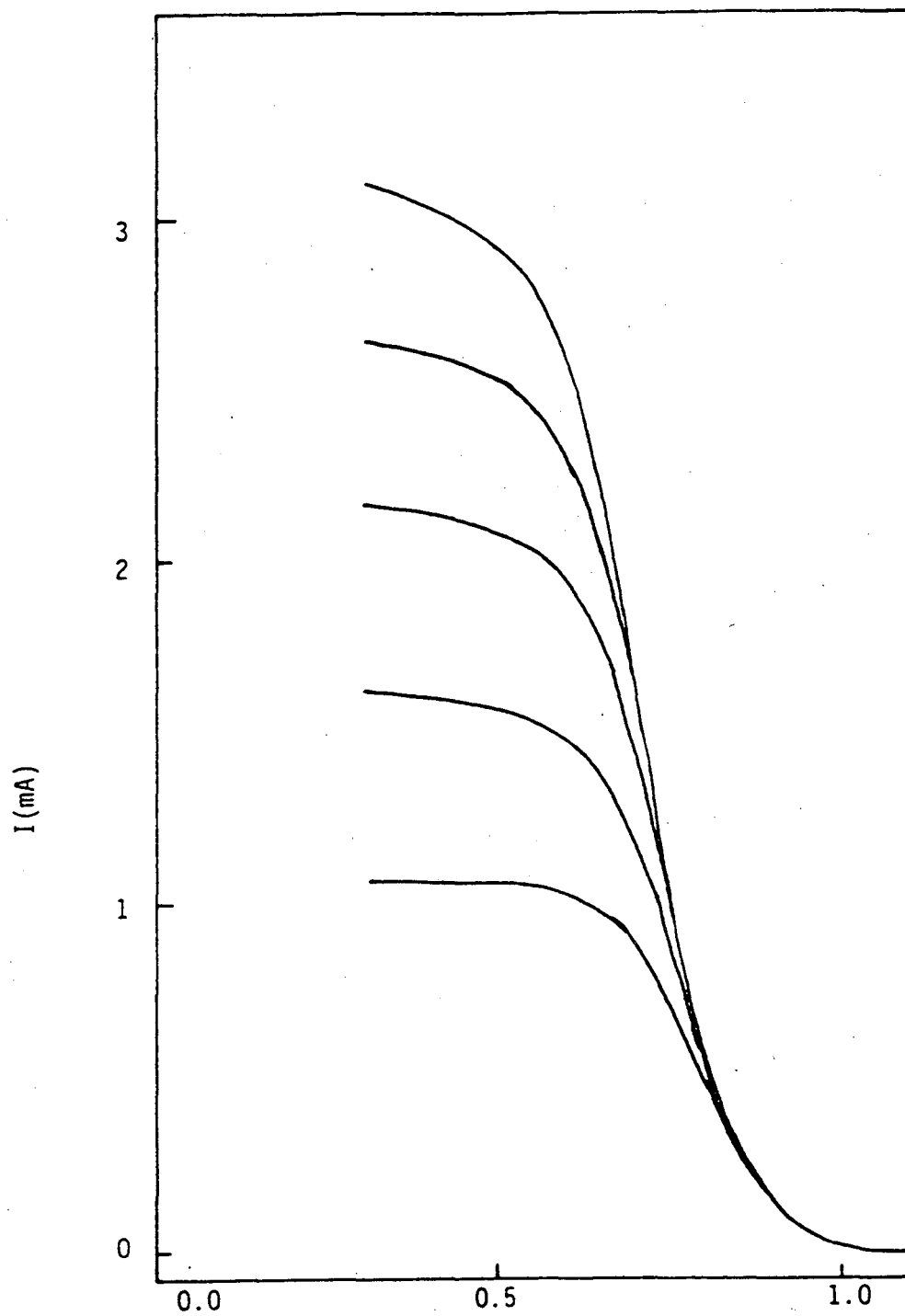


Figure 29 Oxygen reduction on Pt rotating disk electrode in 0.7M H_3PO_4 . Scan rate: 10 mV/sec.

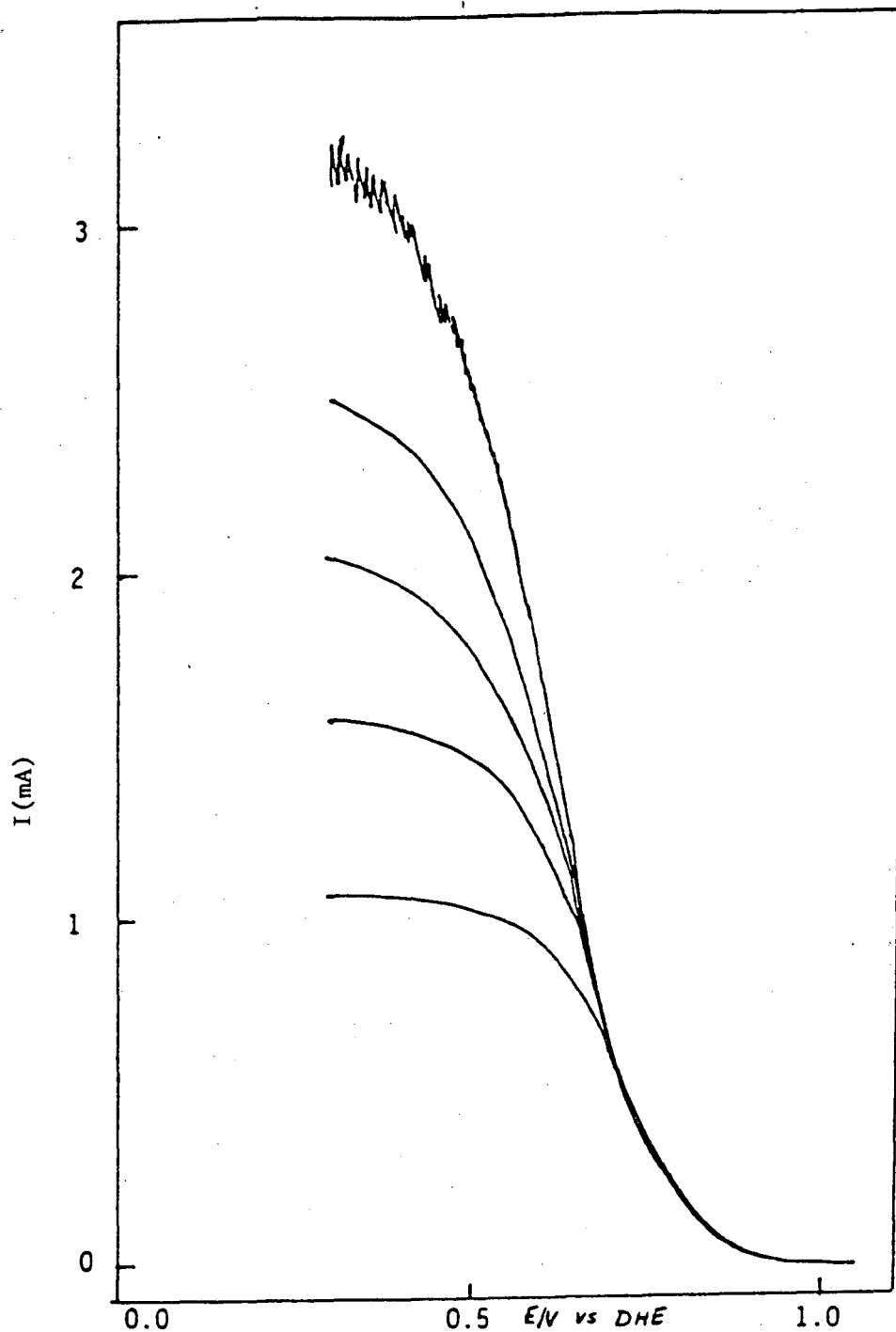


Figure 30 Oxygen reduction on Pt rotating disk electrode in 0.7M H_3PO_4 + 0.01M $C_8F_{17}SO_3H$. Scan rate: 10 mV/sec.

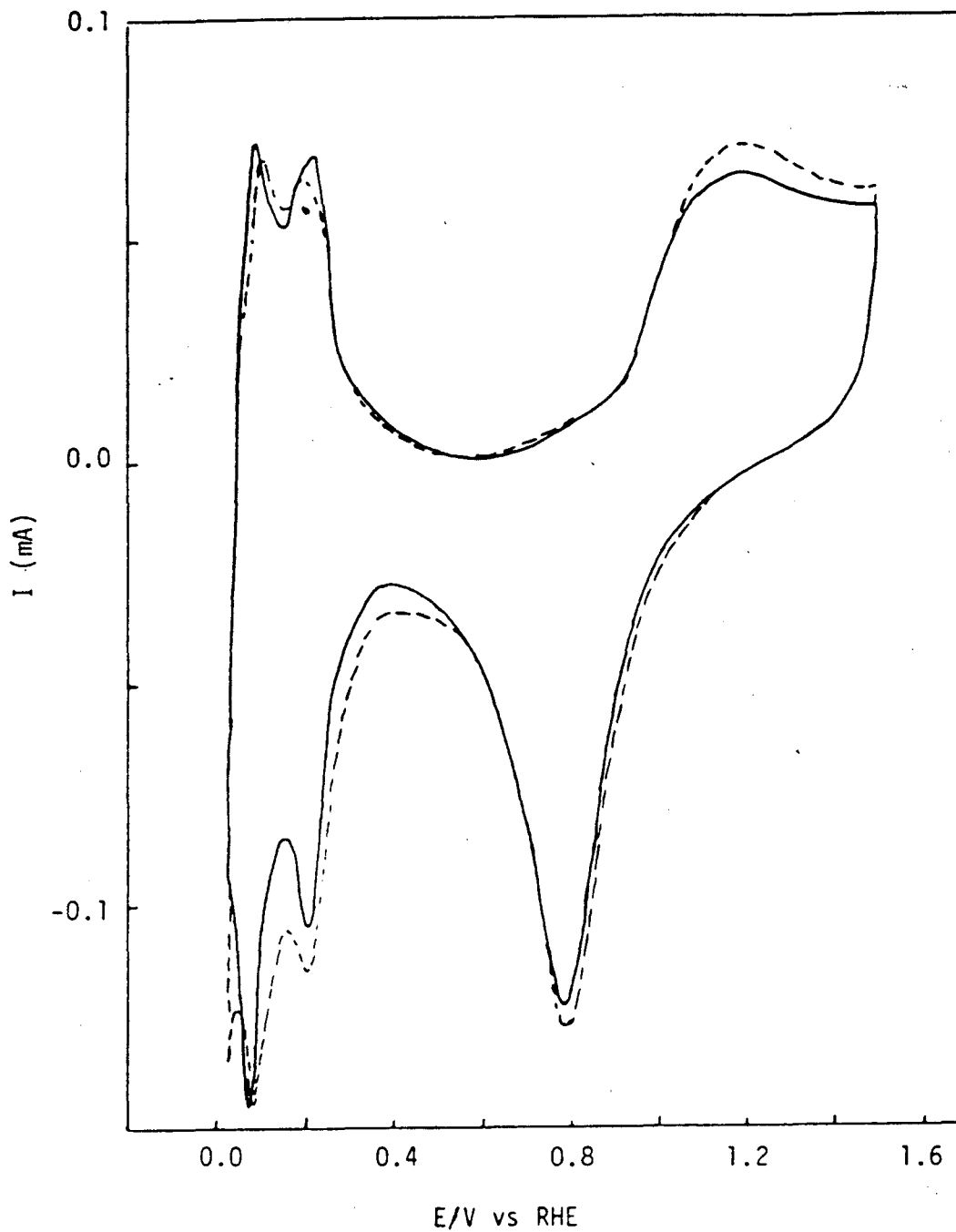


Figure 31 Cyclic voltammograms of Pt in 85% H_3PO_4 (—) and 85% H_3PO_4 + 0.45% $C_8F_{17}SO_3H$ (-----) solutions saturated with N_2 . Scan rate: 100 mV/sec.

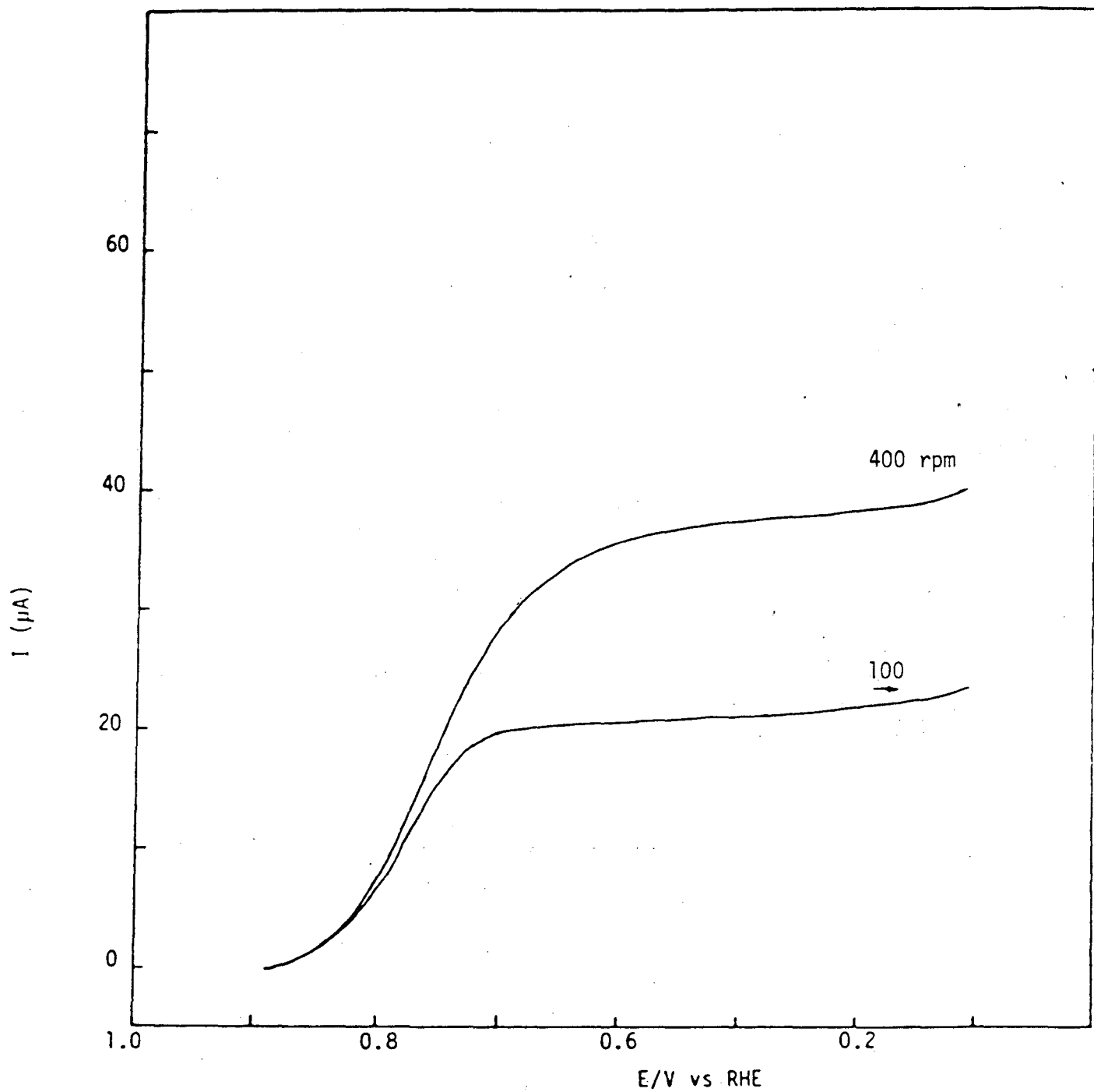


Figure 32 Oxygen reduction on Pt rotating disk electrode in 0.7M H_3PO_4 . Scan rate: 10 mV/sec.

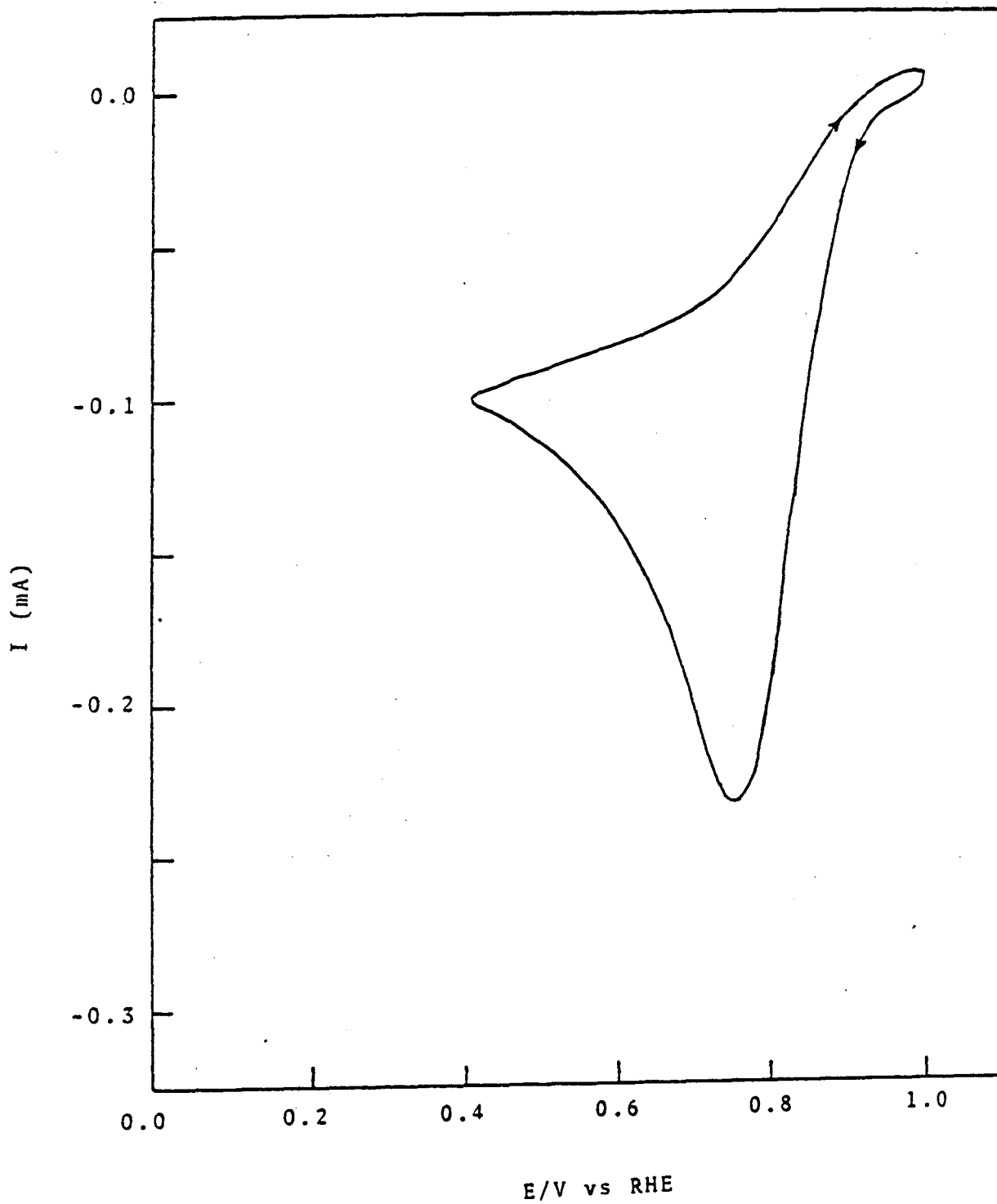


Figure 33 Cyclic voltammogram of Pt in O₂-saturated solution of 0.1M H₃PO₄
Scan rate: 10 mV/sec

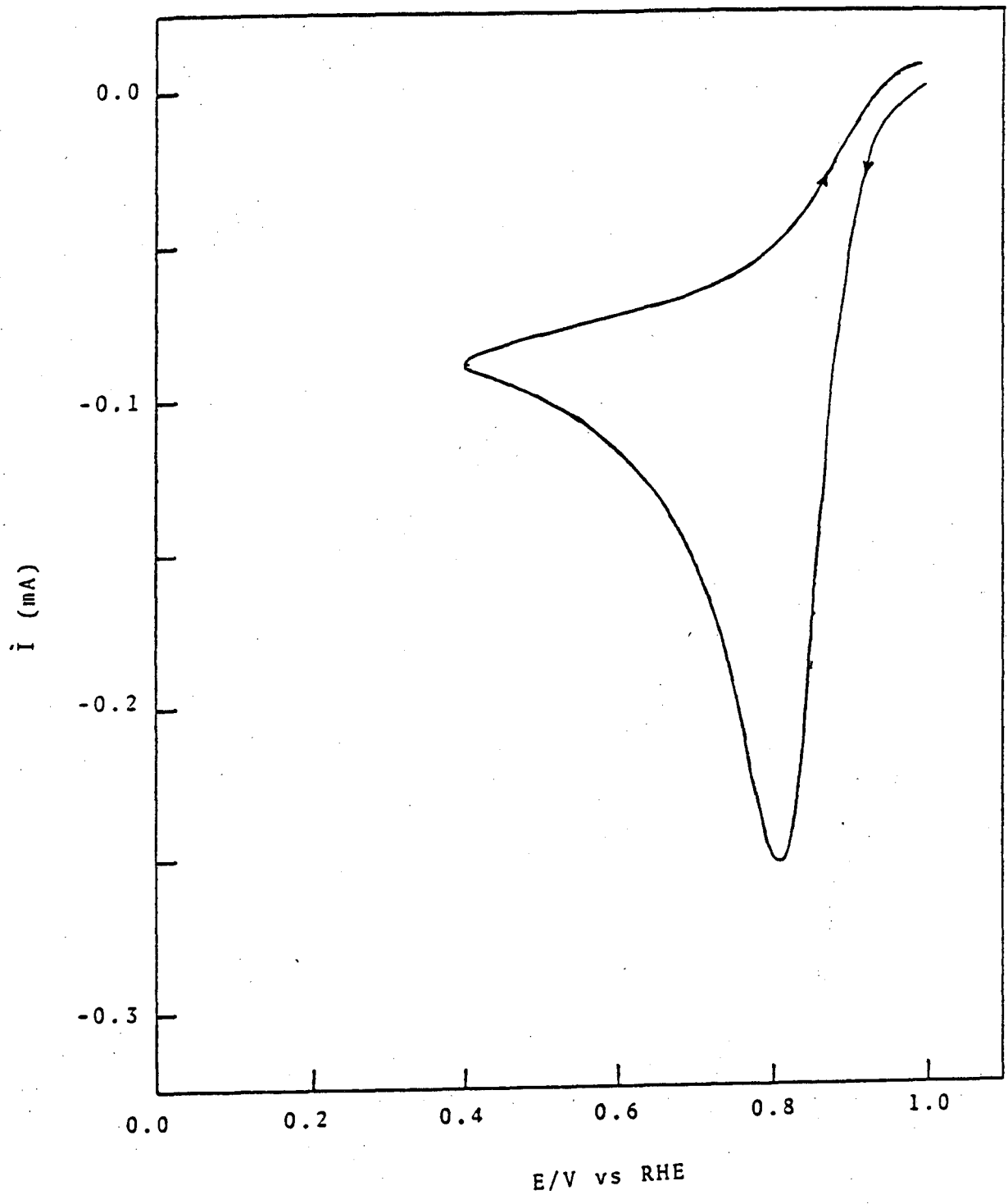


Figure 34 Cyclic voltammogram of Pt in 0.1N $(CF_2)_4(SO_3H)_2$ saturated with O_2 .
Scan rate: 10 mV/sec

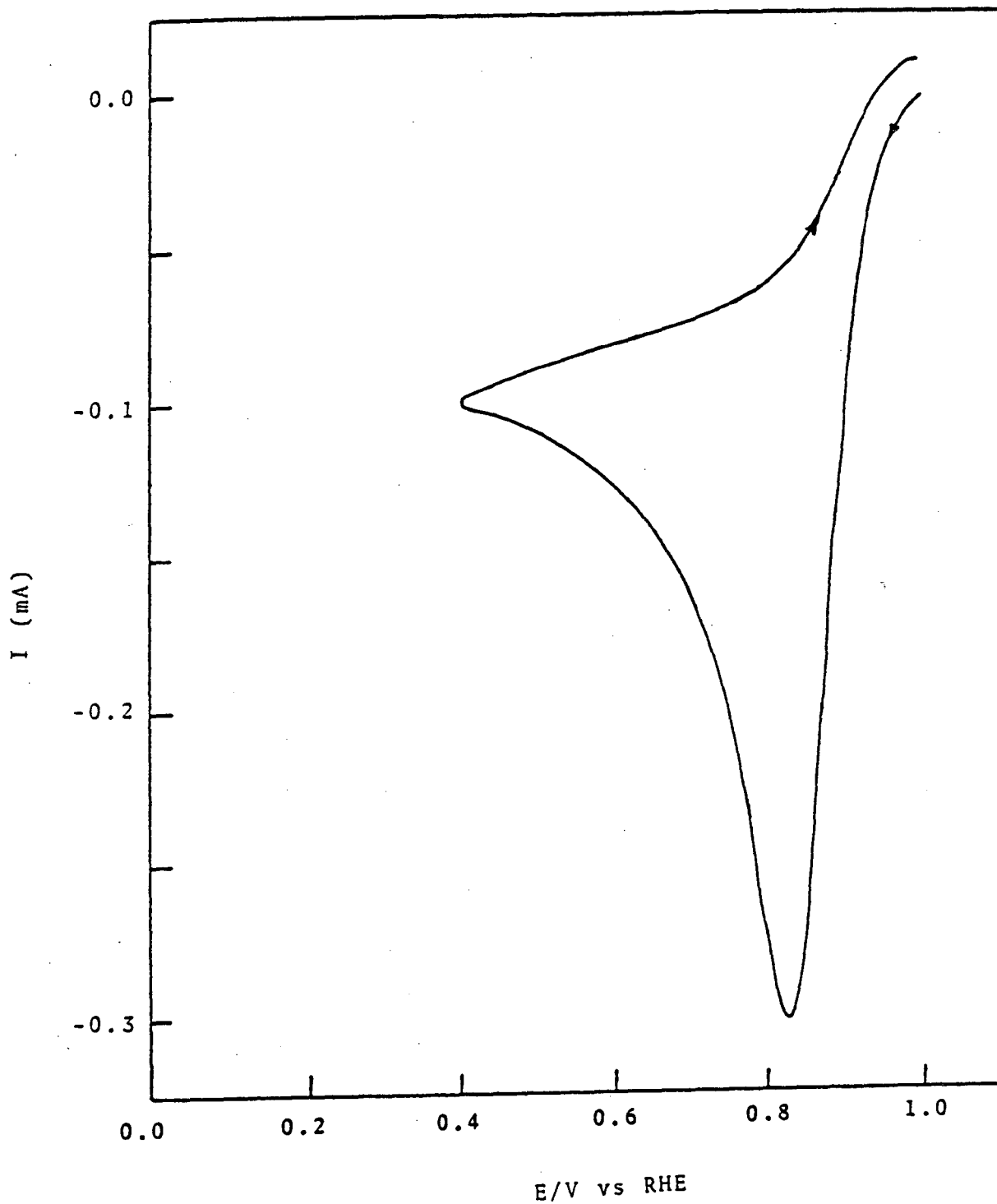


Figure 35 Cyclic voltammogram of Pt in O₂-saturated solution of 0.1M (CF₃SO₂)₂CH₂.
Scan rate: 10 mV/sec

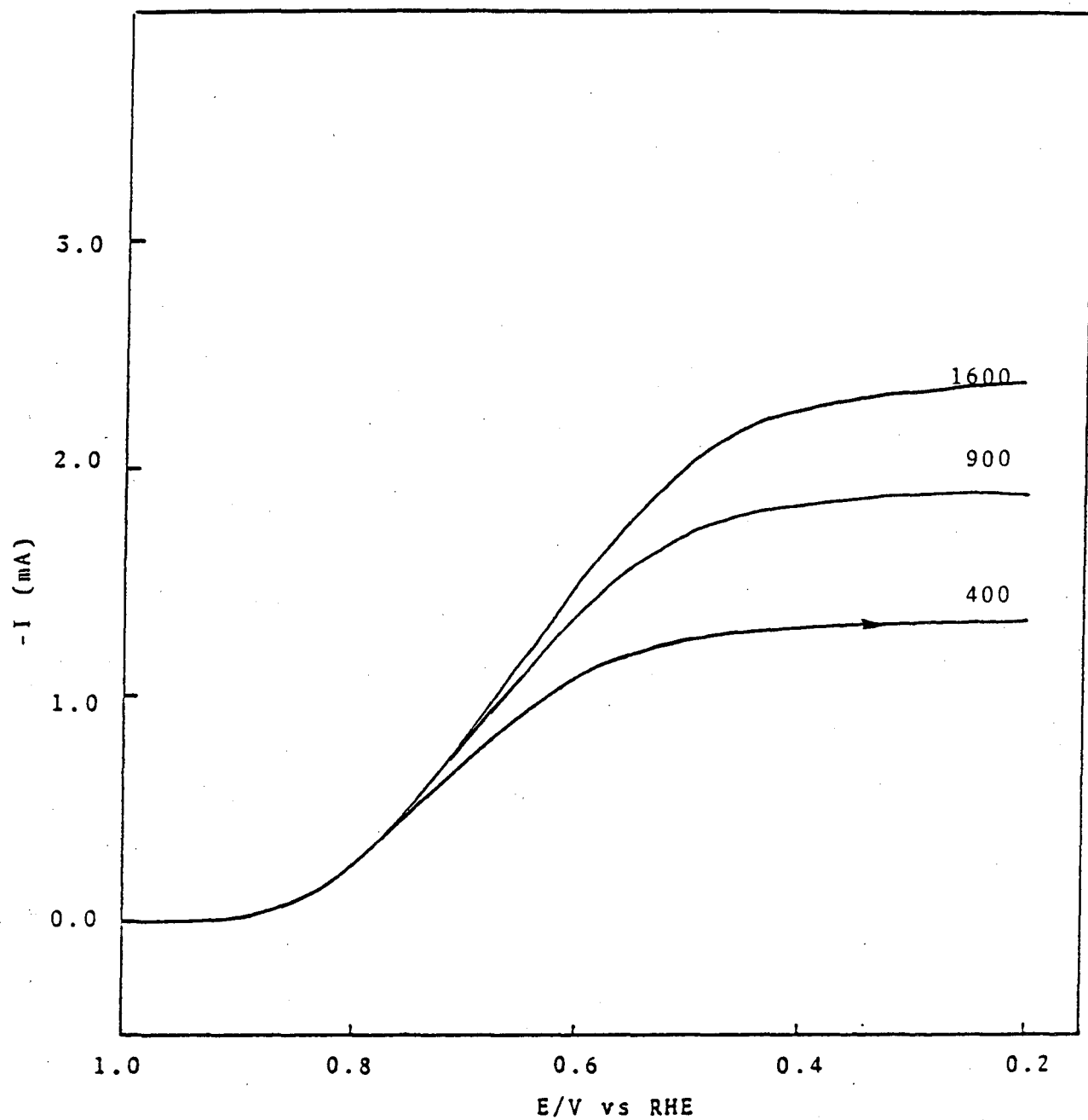


Figure 36 Rotating disk data for O_2 reduction on Pt in $0.1M H_3PO_4$
Scan rate: 10 mV/sec

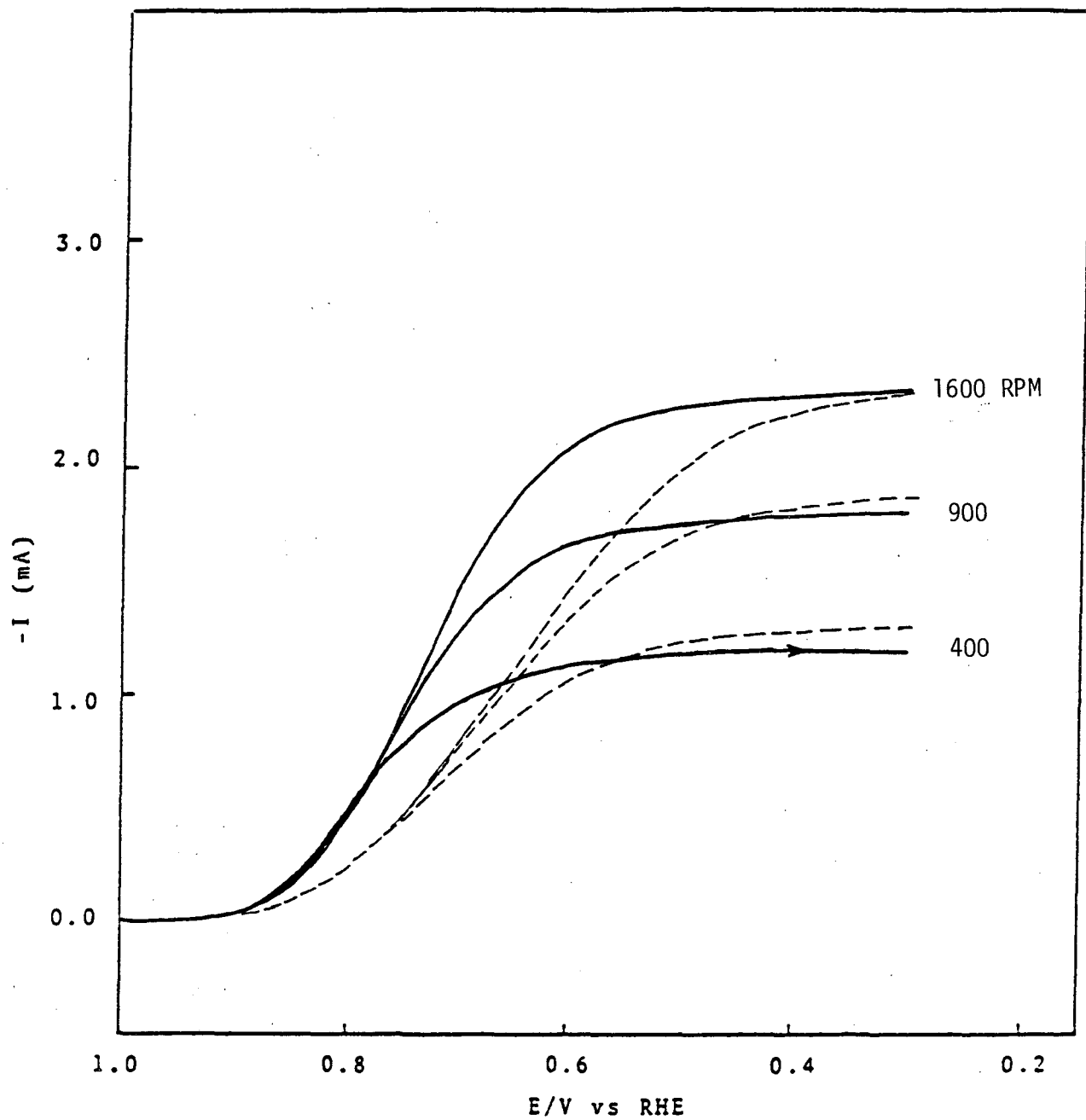


Figure 37 Rotating disk data for O_2 reduction on Pt in 0.1M H_3PO_4 (-----) and 0.1M $(CF_2)_4(SO_3H)_2$ (—). Scan rate: 100 mV/sec.

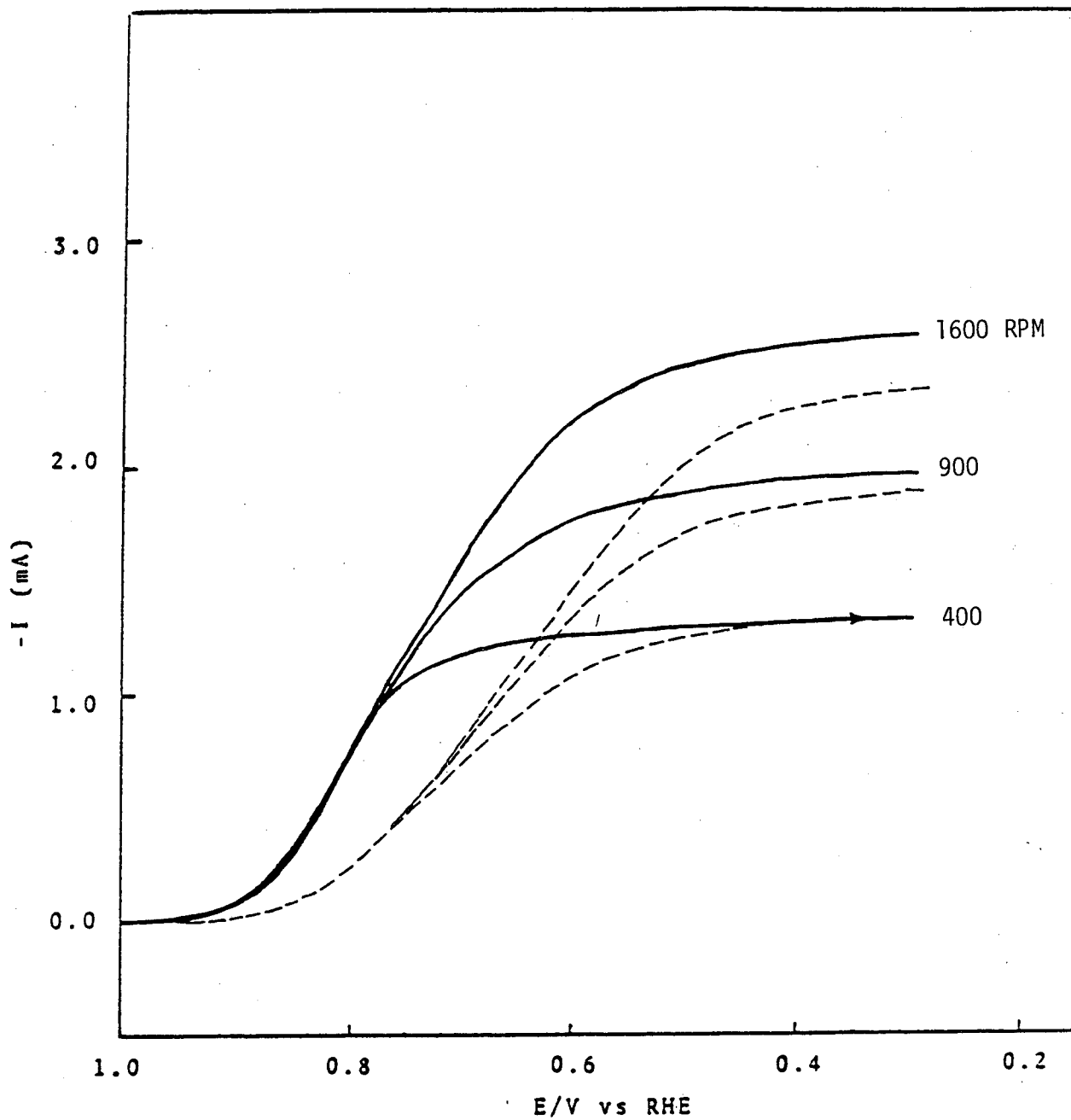


Figure 38 Rotating disk data for O_2 reduction in $0.1M$ H_3PO_4 (-----) and $0.1M$ $(CF_3SO_2)_2CH_2$ (——). Scan rate: 10 mV/sec.

OXYGEN REDUCTION ON HIGH SURFACE AREA Pt (Prototech) AT 100°C.

95

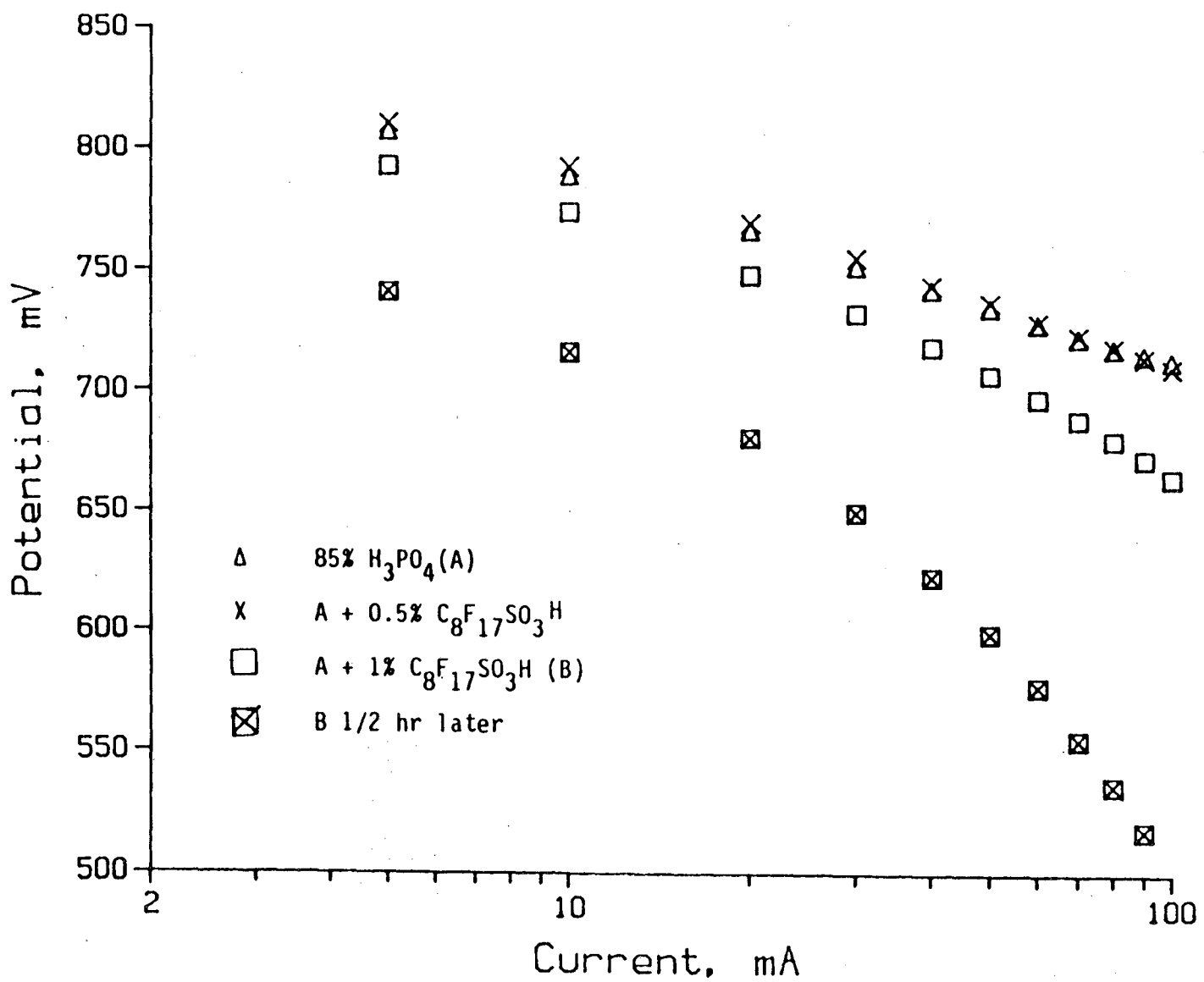


Figure 39

OXYGEN REDUCTION ON HIGH SURFACE AREA Pt (Prototech) AT 100°C.

Δ 85% H₃PO₄
X +2% (CF₂)₆ (SO₃H)₂

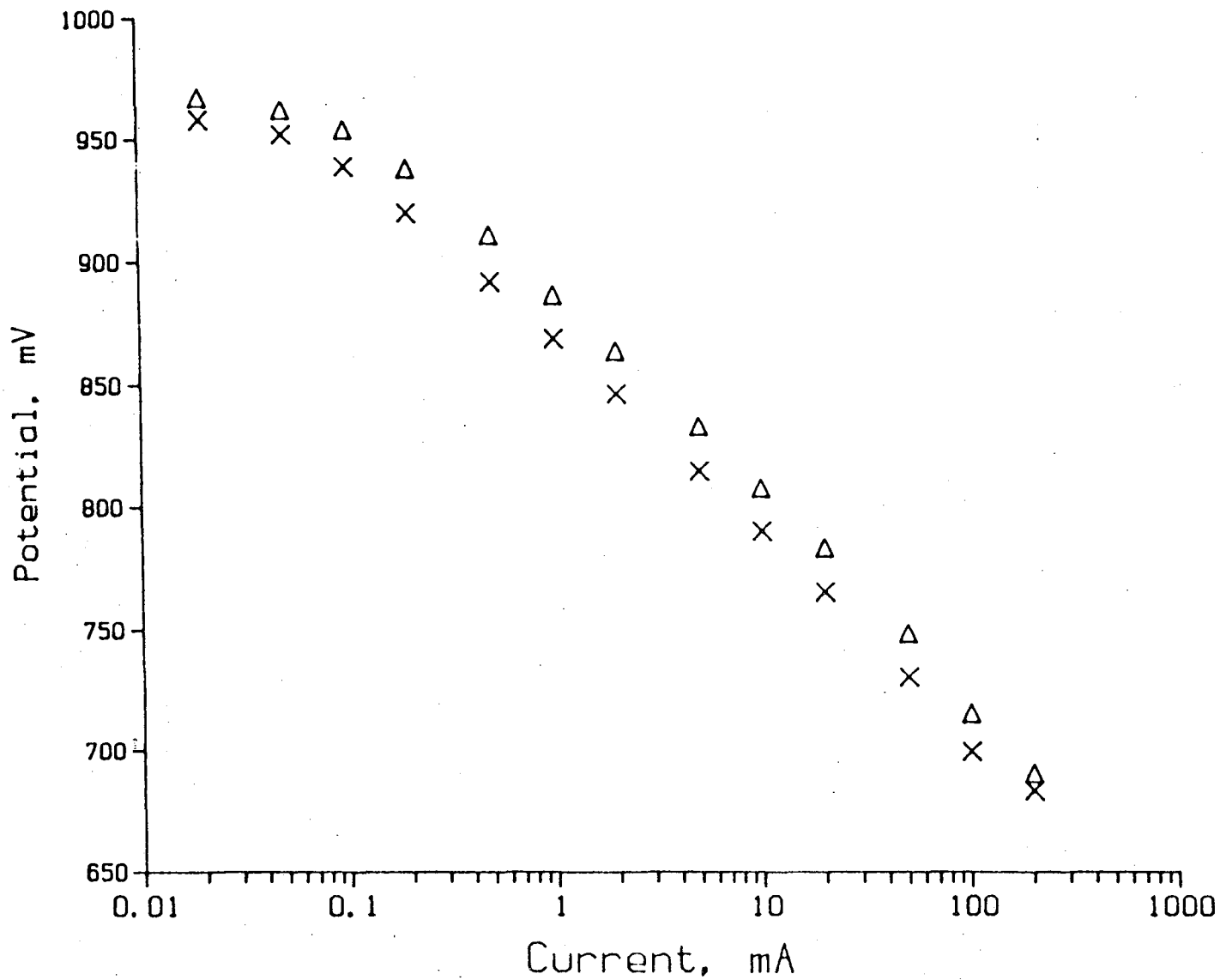


Figure 40

OXYGEN REDUCTION ON HIGH SURFACE AREA Pt (Prototech) AT 100°C.

88

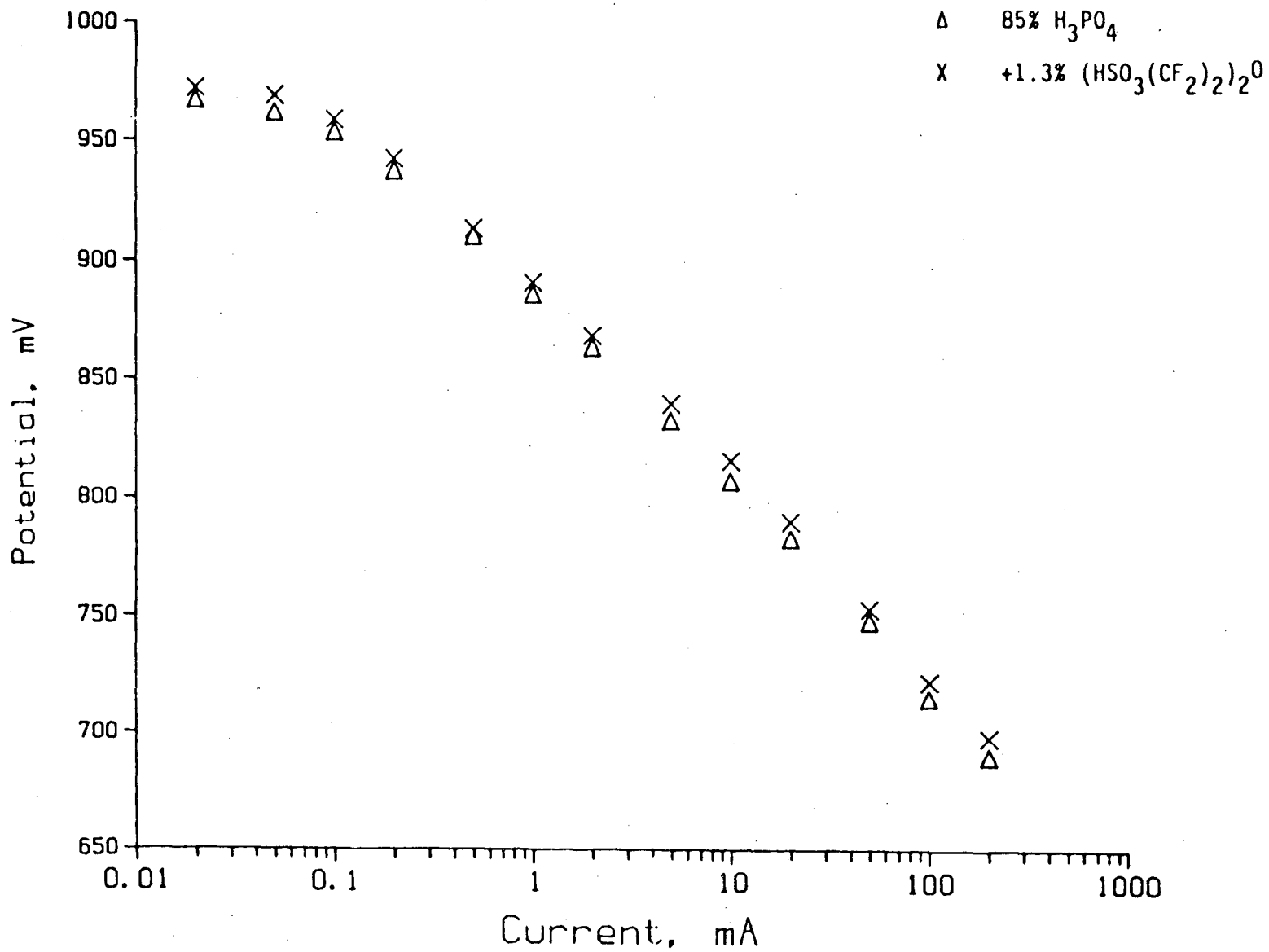


Figure 41

FUEL CELL DATA

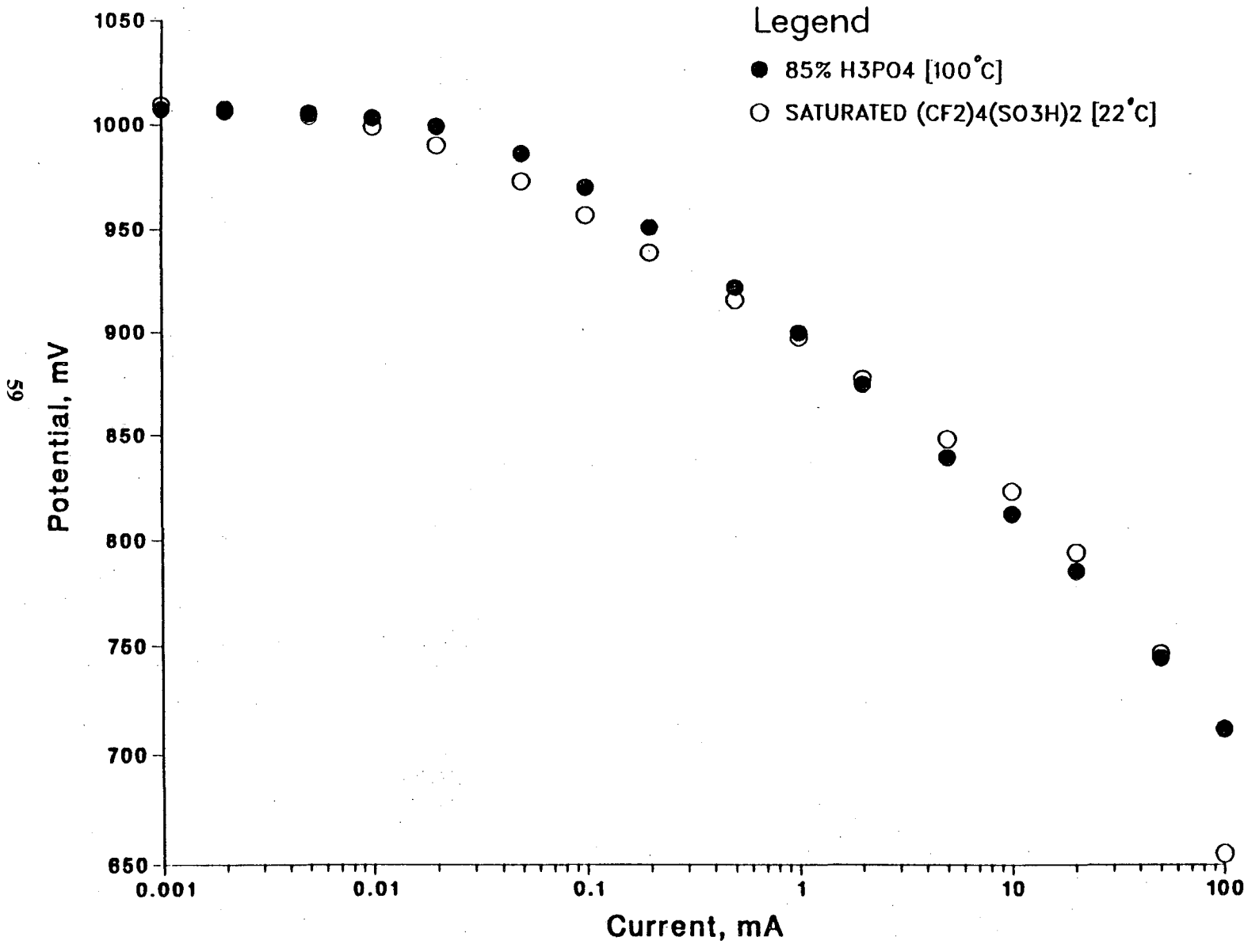


Figure 42

FUEL CELL DATA

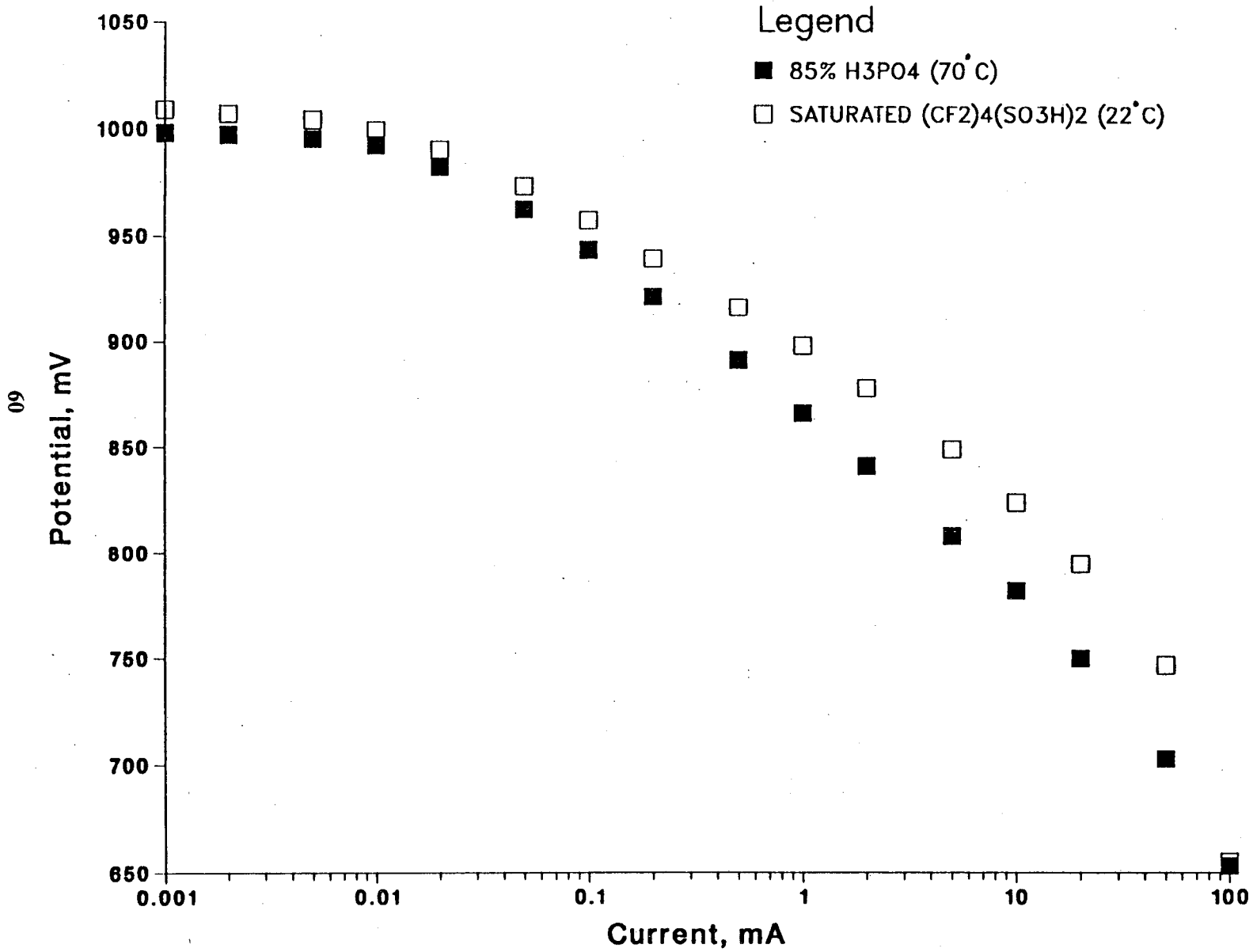


Figure 43

FUEL CELL DATA

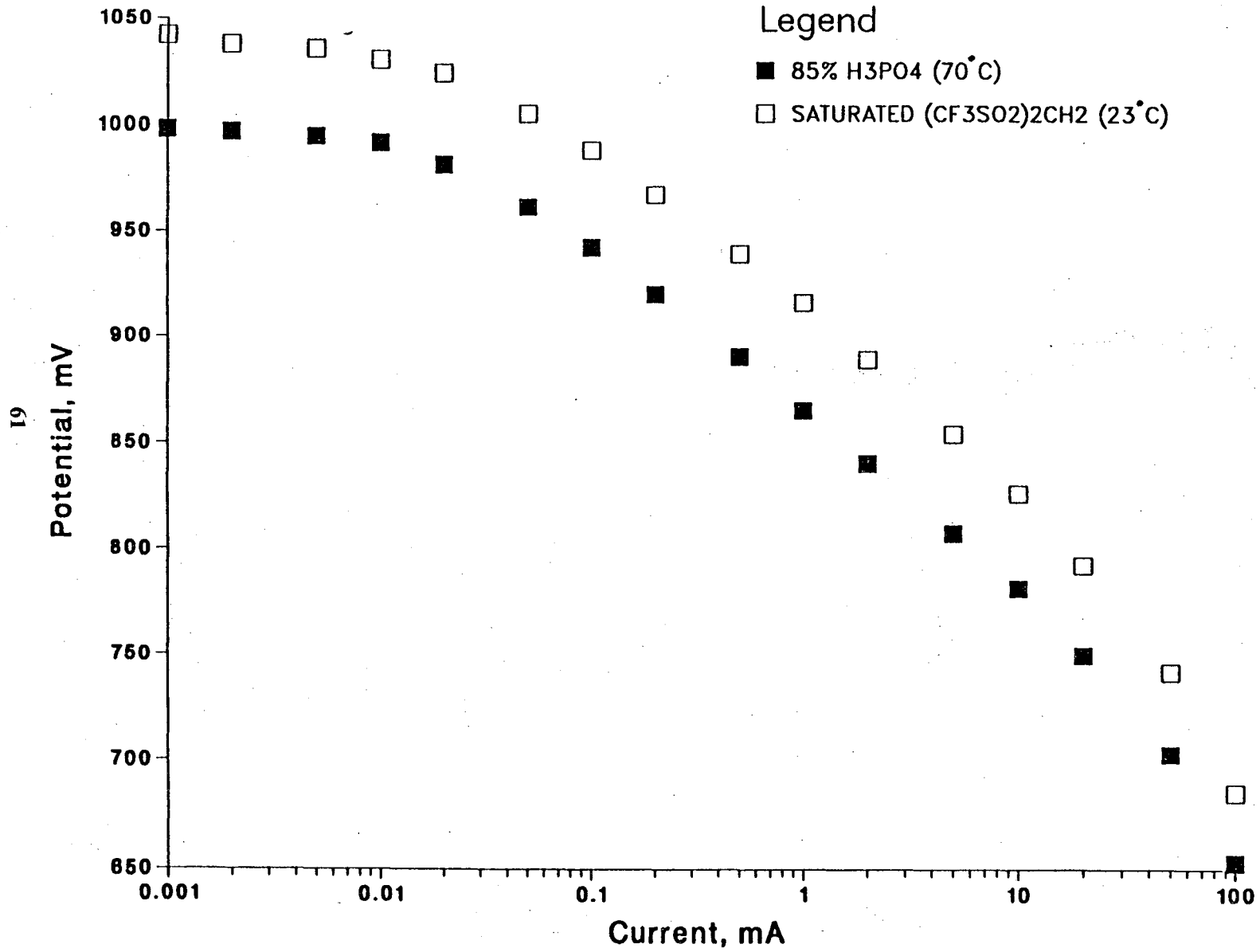


Figure 44

FUEL CELL DATA

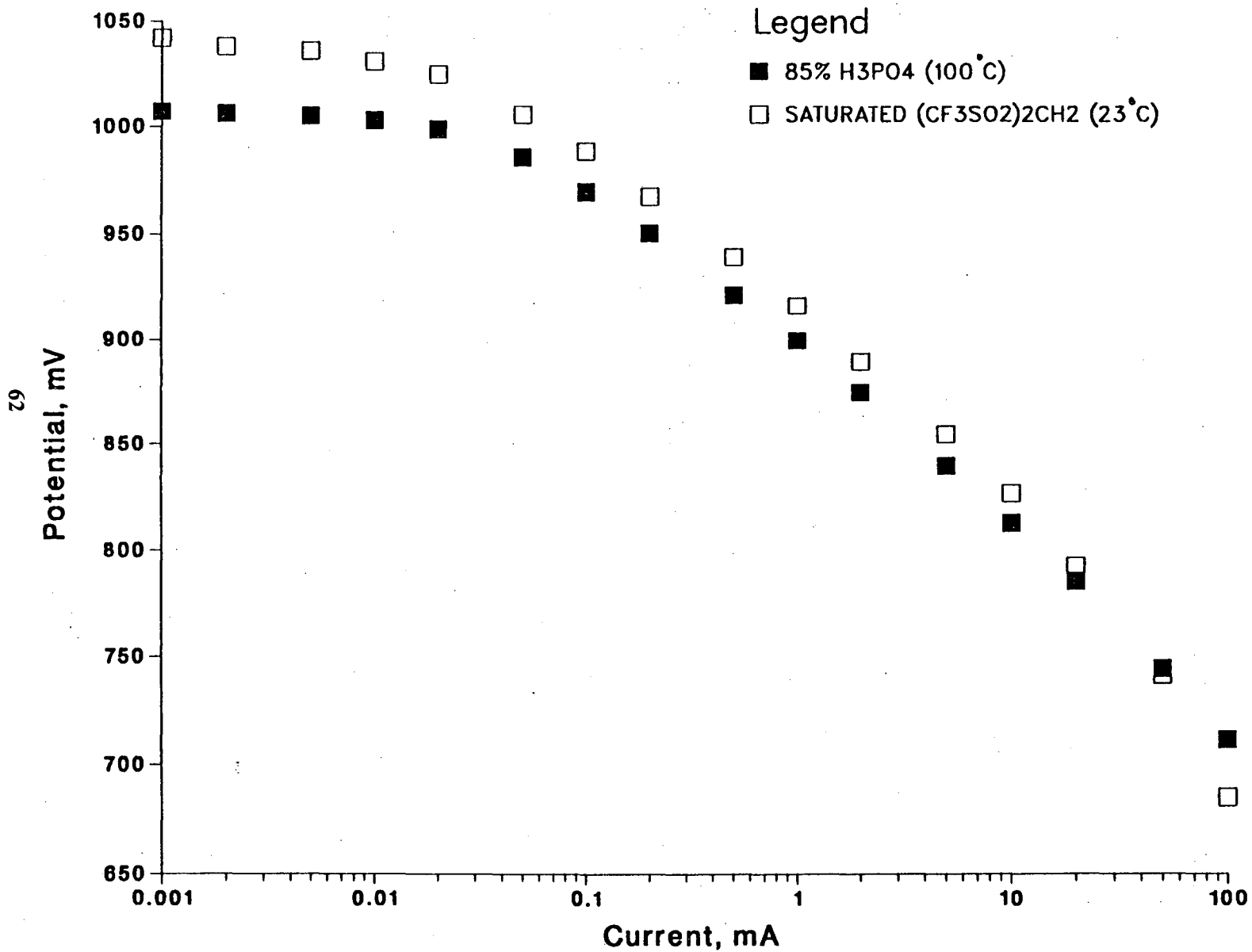


Figure 45

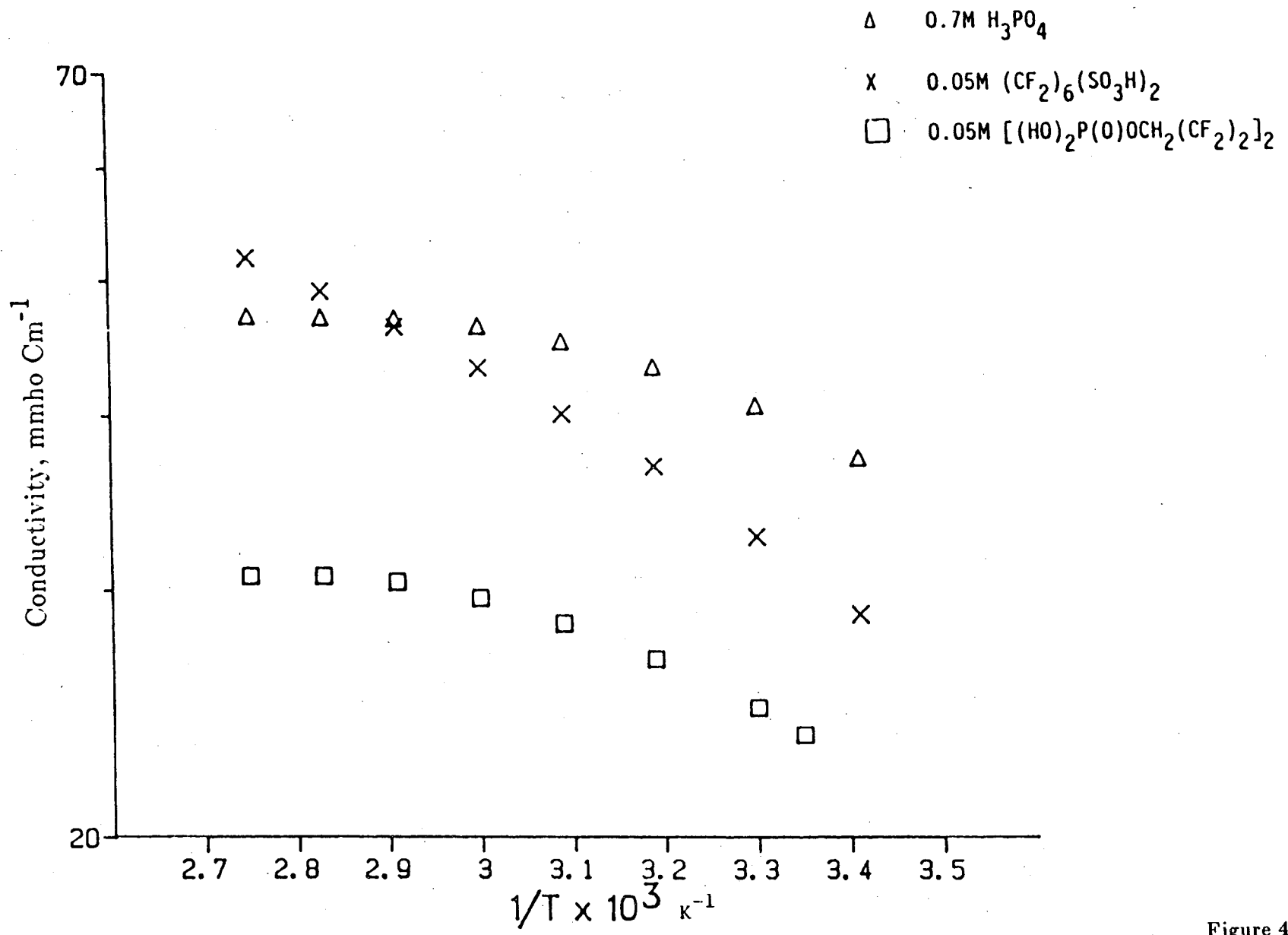


Figure 46

- Δ 0.7M H_3PO_4
- \square 0.12M $SF_5CHFCF_2 SO_3H$
- \times 0.1M $SF_5CH_2 SO_3H$
- \boxtimes 0.05M $(HO_3S(CF_2)_2)_2O$

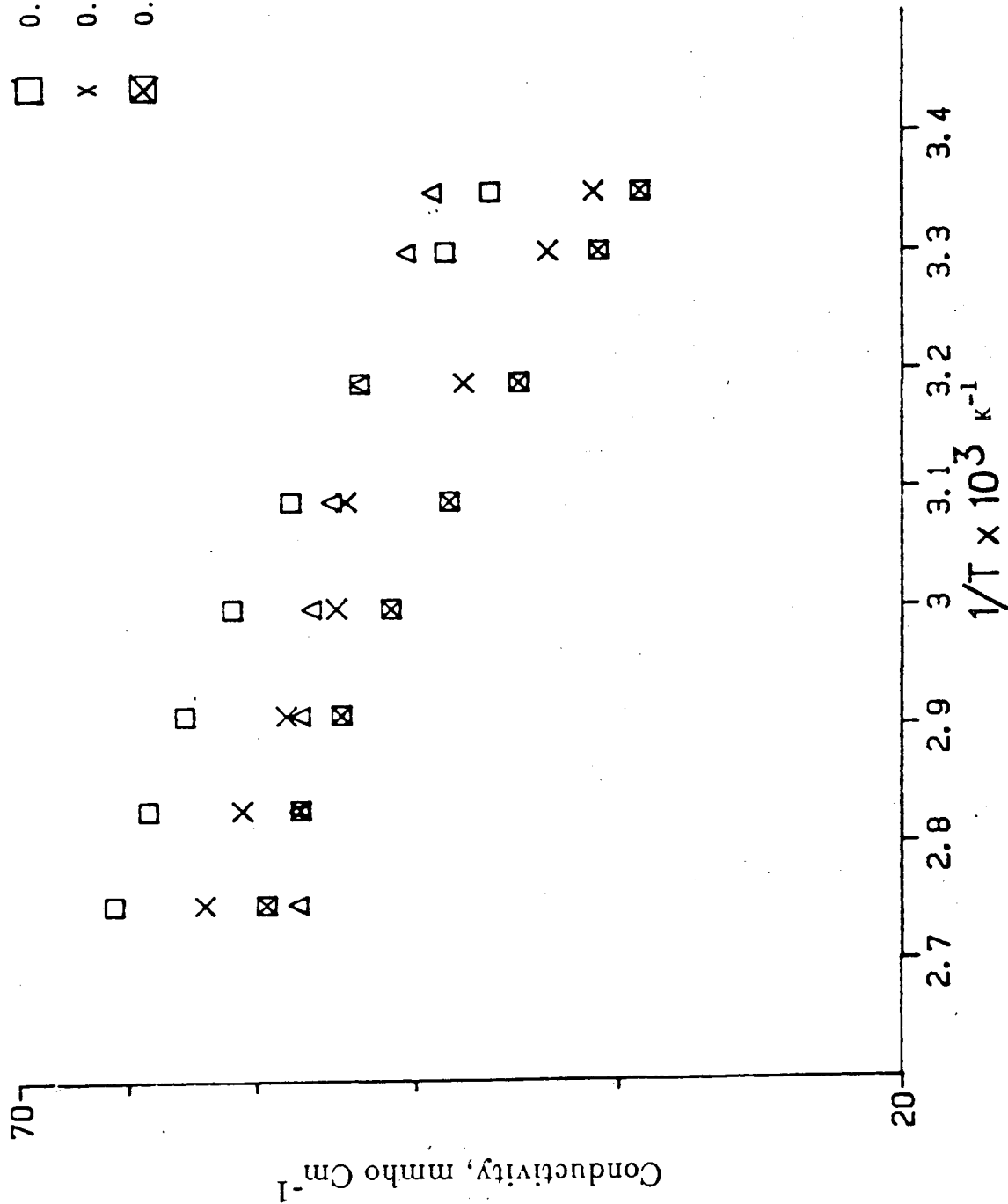


Figure 47

LAWRENCE BERKELEY LABORATORY
TECHNICAL INFORMATION DEPARTMENT
1 CYCLOTRON ROAD
BERKELEY, CALIFORNIA 94720